Journal of Hydrology 645 (2024) 132135

Contents lists available at ScienceDirect

Journal of Hydrology

journal homepage: www.elsevier.com/locate/jhydrol

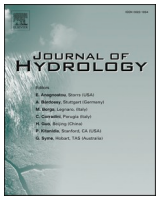

Research papers

Comparative analysis of event runoff coefficients and curve numbers in contrasting urban environments based on observed rainfall-runoff data

Mark Bryan Alivio [a,*], Matej Radinja [a], Mojca Šraj [a], Zoltán Gribovszki [b], Nejc Bezak [a]

[a] University of Ljubljana, Faculty of Civil and Geodetic Engineering, 1000 Ljubljana, Slovenia
[b] University of Sopron, Institute of Geomatics and Civil Engineering, 9400 Sopron, Hungary

ARTICLE INFO

Keywords:
Curve number
Runoff coefficient
Rainfall-runoff
Urban mixed forest
Diurnal cycle
Streamwater viscosity

ABSTRACT

Recently, there has been a growing recognition that the generic values of runoff coefficient (C) and curve number (CN) from standard lookup tables in the literature may not accurately capture the specific characteristics of a given catchment. This study aims to estimate and compare the event C and CN of two contrasting urban catchments in Ljubljana, Slovenia using observed rainfall-runoff data. Estimated parameter values were compared to the tabulated values from the literature (i.e., ASCE, 1992; USDA-NRCS, 2004). Seasonal changes of C and CN, along with diurnal streamflow patterns, were also analyzed to understand the eco-hydrological processes in the urban forest. The results demonstrated that the urban mixed forest exhibited high variability of Cs across all rainfall events with a mean and median of 0.11 and 0.062, respectively. Most of the C values observed in the urban area are clustered around the central tendency with a mean and median of 0.60. These mean C values in both catchments were lower than the tabulated values in the ASCE (1992) design manual. Mean and median CN values in the urban area were 95.45 and 96.81, respectively, lower than the urban mixed forest's CN values of 82.69 and 83.95. An asymptotic CN_{∞} of 90.69 was found for the urban area and 71.71 for the urban mixed forest. Central tendency-derived CN values tend to be slightly higher than the tabulated values from USDA-NRCS (2004) and gridded values from GCN250 (Jaafar et al., 2019), while asymptotic CN_{∞} values were lower. Using central tendency measures as the single lumped value of C and CN may provide a reasonable representation of the runoff behavior in the studied urban area. However, this may present certain challenges in the urban forest catchment. Additionally, pre-event soil moisture conditions and specific storm characteristics contributed to the observed variations in C and CN. Bi-monthly analysis showed that C and CN were high during the autumn and winter months. Diurnal streamflow pattern is most prevalent during low-flow and precipitation-free periods while exhibiting seasonal structures in terms of the shape and timing of maxima and minima. Local estimation of C and CN allows for a more tailored representation of the catchment's hydrological behavior.

1. Introduction

Cities embody a rich mosaic of contrasting urban land uses, from densely built environments with extensive impervious surfaces to green spaces, such as urban parks, forests, street trees, and community gardens, which contribute pervious areas to the urban landscape (Gómez-Baggethun et al., 2013; Rammal & Berthier, 2020). Urbanization creates interconnected networks of impervious surfaces and highly compacted soils (Berland et al., 2017), which significantly impact the local hydrological processes, responses, and functions of catchment ecosystems (Grimm et al., 2008; Hao et al., 2015; Seto et al., 2011; Sun & Lockaby, 2012). Increased surface runoff volumes, high peak flows, and reduction in hydrological losses, e.g., infiltration, interception, and evapotranspiration are some of the major hydrological implications associated with urbanization, exacerbating the challenges in urban stormwater management (Berland et al., 2017). The rainfall-runoff relationships in urban environments also become more complex and highly variable due to the disproportionate distribution of land use patterns, high percentage of impervious surfaces, and variations in soil properties (Li et al., 2018; Miao et al., 2011; Redfern, 2017).

Previous research efforts have focused on advancing our understanding of urban hydrological processes and developing more water-efficient societies with sustainable urban drainage systems. These systems are designed to effectively accommodate and mitigate the impacts

* Corresponding author.
E-mail address: malivio@fgg.uni-lj.si (M.B. Alivio).

https://doi.org/10.1016/j.jhydrol.2024.132135
Received 10 May 2024; Received in revised form 7 August 2024; Accepted 19 September 2024
Available online 10 October 2024

of future extreme rainfall events (Rammal & Berthier, 2020; Thomas, 2017). Among the critical parameters that remain instrumental in understanding the hydrological response of catchments to rainfall events are the runoff coefficient (Machado et al., 2022; Norbiato et al., 2009; Taguas et al., 2017; Xiong et al., 2022) and curve number (Banasik et al., 2014; Lian et al., 2020; Muche et al., 2019). The values of both parameters are typically selected from look-up tables available in the literature and design manuals, which are used as a guide and/or input in designing stormwater drainage systems and other engineering practices.

The runoff coefficient (C) from the rational method represents the fraction of rainfall that becomes direct runoff during a rainfall event (Blume et al., 2007; Machado et al., 2022; Merz & Blöschl, 2009; Norbiato et al., 2009). It is a lumped indicator of runoff generation (Viglione et al., 2009), which is assumed to integrate the effects of land use, soil type, slope, and vegetation (Fassman-Beck et al., 2016). It offers insights into the abstractive and diffusive properties of the catchment (Hayes & Young, 2006) for water resources management, flood control, and water balance analysis (Salazar et al., 2012; Viglione et al., 2009). Studies have found that this parameter exhibits significant variation from location to location and between rainfall events in practice, which often introduces a source of error in the design of hydraulic networks for urban areas, as it is rarely accommodated in the design procedure (Fassman-Beck et al., 2016; Thomas, 2017). The analysis conducted by Velpuri and Senay (2013) on the long-term trends of rainfall and runoff revealed that 12 out of the 21 major urban centers in the United States showed an increasing trend in the runoff coefficients and attributed this observation to the combined influence of human intervention and climate. Similarly, the study by Birkinshaw et al. (2021) on 20 highly urbanized and 5 rural catchments in the UK demonstrated that urban catchments show significant variability in the monthly runoff coefficient between catchments, while rural catchments have a similar response.

Curve number (CN) is a dimensionless index used to characterize the runoff potential of a specific land area due to a given rainfall event (Deshmukh et al., 2013; Gonzalez et al., 2015; Hawkins et al., 2008; USDA, 1986). It is a function of hydrologic soil group, land use/land cover, slope, and antecedent soil moisture (Deshmukh et al., 2013; Hawkins et al., 2008; Lian et al., 2020; Muche et al., 2019; USDA-NRCS, 2004; USDA, 1986). It is employed in the Soil Conservation Service Curve Number (SCS-CN) method, a widely used hydrological method for estimating and predicting direct runoff from small agricultural and natural catchments, which is later adapted to urban catchments (Banasik et al., 2014; Boughton, 1989; Hawkins et al., 2008; Soulis et al., 2009; Wilson et al., 2017; Woodward et al., 2006). Several studies have concluded that CN values obtained from observed rainfall-runoff data provide better estimates of runoff from a given land use compared to the tabulated CN values (Banasik et al., 2014; Gonzalez et al., 2015; Ibrahim et al., 2022; Lal et al., 2017; Lian et al., 2020; Singh & Mishra, 2019). Banasik et al. (2014) reported that the CN values estimated from recorded rainfall-runoff events in a small urban catchment in Poland exhibit large variations and suggested that the application of mean CN for design flood estimation can be problematic. The work of Gonzalez et al. (2015) has shown that there is a better agreement between the simulated and observed runoff when the empirical CN is adjusted to account for the changes in vegetation than using the standard CNs from the look-up tables without further adjustment.

Hydrologists, researchers, and engineers often face a degree of ambiguity regarding the selection of C and CN values from standard look-up tables, which is a common practice for hydrological analysis and engineering design (Lian et al., 2020; Thomas, 2017; Viglione et al., 2009). They need to rely on their judgment and experience to select the most appropriate values for the specific catchment and purpose they are working on. This ambiguity stems from the fact that these values are based on generalized assumptions and average conditions and inevitably fall short in capturing the site-specific characteristics of the catchment (Dhakal et al., 2012; Thomas, 2017; Young et al., 2009; Zhang et al., 2014), particularly in urban environments where a wide range of land uses and impervious surface properties exists. Additionally, the look-up table values may not be up-to-date, as climate change, urbanization, and other factors can lead to changes in catchment characteristics and runoff behavior. Thus, obtaining the C and CN through direct observation and analysis of rainfall-runoff events enables tailoring these parameters to the local conditions of the catchment, providing a more accurate and representative assessment (Hawkins, 1993; Lal et al., 2017; Thomas, 2017).

In recent years, there has been a growing recognition of the need for site-specific data and parameters to characterize the hydrologic response and behavior of the catchments. The study aims to estimate and compare the event runoff coefficients and curve numbers, derived from recorded rainfall-runoff data of two contrasting environments in Ljubljana, Slovenia: urban mixed forest and highly impervious urban area. Analyzing both C and CN together is an approach that, to our knowledge, has not been extensively undertaken in previous studies. These parameters have been analyzed independently due to differences in conceptual basis, data requirements, and application scopes. However, a dual analysis of C and CN for each catchment offers a complementary insight into the hydrological processes at play in urban environments, particularly in the estimation of runoff, as each method has its own limitations and strengths. This research also explores the variability of C and CN across different urban environments and rainfall events, which provides a more integrated understanding of these hydrological indices. The estimated C and CN values are then compared to the tabulated and gridded values available in the literature (i.e., ASCE, 1992, 1996; GCN250 by Jaafar et al., 2019; USDA-NRCS, 2004). Furthermore, another particular interest that we examined is the seasonal change of C and CN according to the phenological season of tree canopies, namely the growing and dormant seasons. Specific to the catchment in the urban mixed forest, we also analyzed the diurnal cycles of the streamflow to gain a better understanding of the eco-hydrological processes occurring in the urban forest and its intricate response to environmental drivers. Through this research, we aim to contribute to the growing body of knowledge in urban hydrology and the development of empirical and locally tailored parameters to improve urban hydrological modelling and the accuracy of surface runoff predictions. The findings from our study can be used to refine the calibration of C/CN in machine learning models, e.g., the rainfall-runoff models developed by Radinja et al. (2021) using machine learning, where CN is one of the calibrated parameters. This contribution holds particular relevance for urban planners and water resource managers, as it aids in the design of effective urban stormwater management strategies and the integration of green infrastructures in cities that are grounded in the specific hydrological behavior of a catchment.

2. Study area

For this study, the two experimental catchments with different land use/land cover properties and hydrological regimes were selected: (1) urban mixed forest and (2) highly impervious urban areas. The catchments are located within the urban area of Ljubljana, Slovenia, as shown in Fig. 1. The city is characterized by a favorable balance of open (green) spaces and built-up areas, contributing positively to both the quality of life and ecosystems (Krevs et al., 2010). A distinctive feature of Ljubljana's urban structure is the presence of extensive green spaces accounting for almost 75 % of the city's surface area which consists primarily of green wedges stretching to the city center (Nastran & Regina, 2016). The climate regime of the study location is temperate continental with a mean annual rainfall of 1371 mm and mean annual temperature of 11 °C based on the long-term meteorological data (1970–2022) at the Ljubljana-Bežigrad synoptic station. Records of the average daily temperature between 1970 and 2022 show a statistically significant increasing trend, while rainfall exhibits an inter-annual variability and increased occurrence of extreme seasonal conditions. On average, more than 50 % of the mean annual rainfall is being

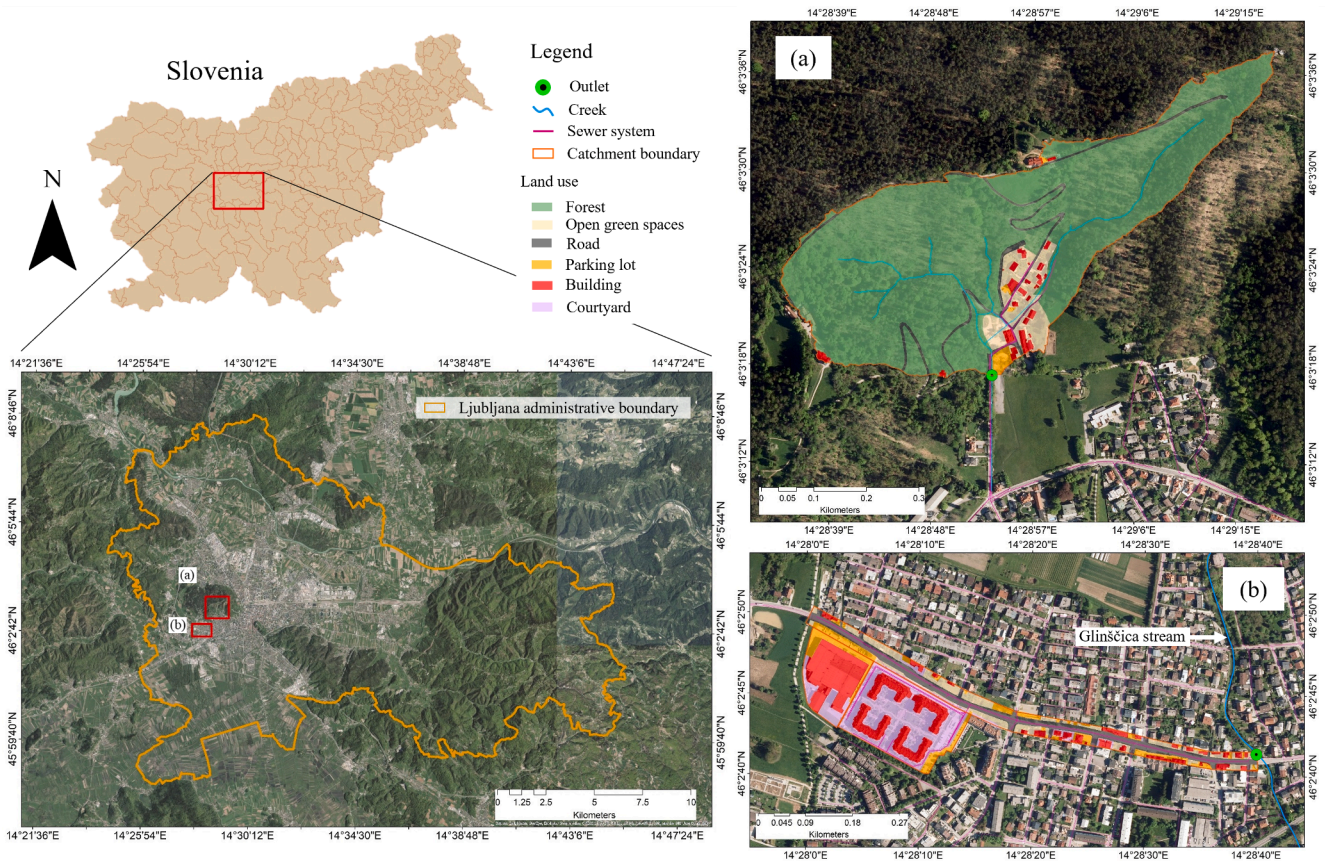

Fig. 1. Location and land use of the studied catchment: (a) urban mixed forest in Rožnik hill and (b) urban area in the city of Ljubljana, Slovenia.

delivered during summer and autumn (ARSO, 2023). Research on the rainfall-runoff processes in both catchments is crucial in the context of urban stormwater management in a changing climate and environment.

The studied urban mixed forest lies within the landscape park of Tivoli, Rožnik and Šiška Hill, a protected area of high nature value in the vicinity of Ljubljana city center. Due to their immediate proximity to the city, Ljubljana's urban forests are of critical importance to the city population for leisure activities and recreation, including tourism. In addition to this, urban forests offer several environmental benefits to the city, such as regulating the local climate, reducing air and noise pollution, mitigating the urban heat island effect, and managing stormwater runoff, among others. Hence, the delineated catchment (Fig. 1a) in this study, with an area of 0.24 km^2 and an average slope of 38.3 %, is nourished by Rožnik hill with an outlet discharging into the city's drainage system. Therefore, the municipality has recognized the opportunity and importance of minimizing runoff discharge in wet periods while promoting water retention during dry periods through the implementation of nature-based infrastructures. Moreover, the catchment has a dense forest cover from the mixed canopies of sessile oak (*Quercus petraea (Mattuschka) Liebl.*), sweet chestnut (*Castanea sativa (Mill.)*) and Norway spruce (*Picea abies (L.) Karst.*), making it the dominant land use in the area. In general, the percentage share between deciduous and coniferous trees in the growing stock was 54 % deciduous trees and 46 % coniferous trees. The study on rainfall partitioning in this urban mixed forest showed that the average annual canopy interception was 18.0 % of the gross precipitation and the seasonal variation was nearly identical throughout the year, with a 2 % lower interception during the growing (leafed) season compared to the dormant (leafless) season (Kermavnar & Vilhar, 2017). Additionally, the volumetric soil moisture was measured at 3 different depth profiles (16–20, 51–54, 74–76 cm) in the open area and under the forest canopies using the TEROS 10 sensor from METER Group (Inc.) with an accuracy of ± 3 %. However, for this study, only the response of the upper soil profile (16–20 cm) to each rainfall event was considered and shown for the analysis. Thus, according to the laboratory analysis of the soil samples from both locations, the soil in most of the identified depth horizons is classified as silty clay loam.

In contrast, the second location (0.078 km^2, average slope of 7.1 %) is a highly urban area (Fig. 1b) on the western side of Ljubljana with a large percentage of impervious surfaces from buildings, roads, parking lots, etc. The predominant land use in this area is a mix of residential and commercial uses with dispersed patches of small-scale open green spaces (e.g., gardens, grass lawns, trees). The soil type in the area is typical urban soil (e.g., human-altered and human-transported) with no additional information about soil characteristics aside from artifactual materials from brick particles, concrete debris, ceramics, etc. (Radinja et al., 2019). Soil analysis of nearby parks and locations within the vicinity of Ljubljana shows that the soil ranges from sandy clay loam (e.g., Radinja et al., 2019; Svetina et al., 2023) to silty clay loam (e.g., Radinja et al., 2019). This location was selected because the area is served by a separate drainage system for stormwater and wastewater, as well as, due to its proximity (< 2 km) to the urban mixed forest. The stormwater runoff from this catchment is directly discharged into Glinščica stream, which feeds into the larger Gradaščica river, both of which have a history of causing flooding in surrounding urban areas of the Vič district of Ljubljana (Bezak et al., 2018; Rusjan et al., 2003). Also, the city's drainage systems are not designed to deal with the escalating frequency and intensity of heavy rainfall events, often resulting in capacity constraints and elevated risks of sewer overflows. Consequently, it causes localized inundation of roads, street underpasses, and even garages in the city, particularly during high-intensity storms, thus underscoring the need for effective stormwater management strategies.

Both catchments are representative examples of broader urban settings: one reflects naturally existing urban green spaces while the other has dense urbanization footprints. These contrasting characteristics allow for a comparative analysis and selecting these areas addresses practical urban management concerns. The urban mixed forest was chosen as it represents urban green spaces, which are increasingly being recognized as an element of nature-based solutions in cities to mitigate several environmental impacts (e.g., flooding, air pollution, urban heat island effect). While the second catchment exhibits characteristics and conditions that are commonly found in many urban centers, where stormwater runoff is a significant concern, often overwhelming drainage capacity during heavy rainfall events. To address this predicament, sustainable urban drainage systems have been recognized as an alternative and complement to the conventional approach by taking into account other important aspects of urban water management (e.g., runoff quality, amenity, ecology, etc.). Hence, to achieve optimal efficiency of the design, it becomes imperative to acquire site-specific hydrological parameters, such as C and CN.

3. Data and Methodology

The flowchart in Fig. 2 summarizes the methodological approach for estimating C and CN based on measured rainfall-runoff data. It outlines the key steps involved in the analysis, from data collection and preprocessing to the calculation of representative hydrological parameters and comparison to the generalized tabulated values.

3.1. Rainfall-runoff measurements

In the scope of this study, we analyzed 86 rainfall-runoff events that occurred in both catchments during the investigated period from August 2021 to August 2023. Rainfall was measured at 5-minute intervals using a tipping bucket (0.2 mm/tip) rain gauge (Onset RG2-M) connected to an automatic data logger (Onset HOBO Event), which was installed in the open area of a small urban park adjacent to the Department of Environmental Civil Engineering building (46.04°N, 14.49°E) (Alivio et al., 2023; Zabret et al., 2018, 2023; Zabret & Šraj, 2021, 2019a, 2019b, 2018). Rainfall events were separated by a minimum 4-hour dry period (Zabret & Šraj, 2018, 2021) and only with more than 5 mm of cumulative amount were considered in the analysis. Additionally, the study period was partitioned into two primary seasons, which are defined according to the phenological phases of deciduous trees, a dominant tree species in Rožnik hill (Kermavnar & Vilhar, 2017): (a) the growing (leafed) period, from May 1 to October 31; and (b) the dormant (leafless) period, from November 1 to April 30.

In the urban mixed forest catchment, a rating curve was used to convert observed water level data to discharge estimates. Water level was monitored at 10-min resolution in a narrow creek at the outlet of the studied catchment using a HOBO Fresh Water Level Data Logger. The logger was secured inside a PVC pipe and installed in such a way that the sensor was approximately 10 cm below the bed of the channel. Raw data from the HOBO logger includes absolute pressure (atmospheric pressure and water head) and temperature readings in 10-min frequency. To compensate for barometric pressure changes, the measurement from an additional logger, deployed 1 m above the top of the creek (in air), was used as a barometric reference. The HOBOware Pro version 3.7.22 software was then used to process and convert pressure readings from the submerged logger into water level information via the barometric compensation tool (do Amaral et al., 2023; Onset Computer Corporation, 2018). Moreover, the stage–discharge relationship (rating curve) was established by performing sporadic discharge measurements in the channel during low- and high-flow events using a tracer dilution method. A total of 30 discharge measurements were used to establish the rating curve. Specific to this catchment, the hydrograph baseflow separation is made by means of a recursive digital filtering method proposed by Lyne and Hollick (1979), which was carried out with the use of grwat package version 0.0.2 (Samsonov et al., 2022) in R software (R Core Team, 2021). The direct runoff (or event flow) was then calculated by dividing the direct runoff volume by the considered catchment area.

As for the runoff in the urban catchment area, a Doppler area velocity sensor (OCM-KDO-KAPTOR Module, B.M. Tecnologie Industriali, Italy) equipped with the KAPTOR Multi datalogger was installed inside the stormwater drainage pipe, with a diameter of 800 mm. Flow velocity was measured based on the principle of the Doppler effect, with the reflection of ultrasound by moving particles or bubbles in a fluid flowing through the pipe. The water level inside the pipe was measured with the built-in hydrostatic level sensor. The frequency of water level and velocity measurements was set to 5 min. Then, the flow inside the pipe was calculated by combining the information of water velocity, water level, and the geometry of the pipe (B.M. Tecnologie Industriali s.r.l., 2020).

3.2. Estimation of runoff coefficient and curve number from recorded rainfall-runoff data

3.2.1. Runoff coefficient

The runoff coefficient is a widely used and frequently reported

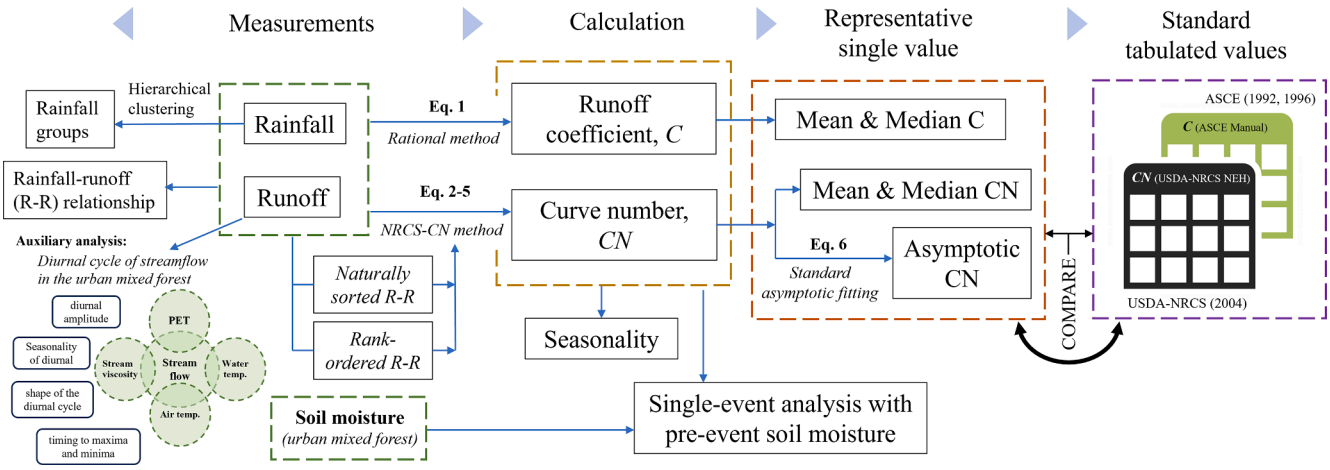

Fig. 2. Methodological flowchart for estimating C and CN using observed rainfall-runoff data.

parameter characterizing the hydrologic response of a given catchment, either on an annual or an event basis (Blume et al., 2007; Merz & Blöschl, 2009; Norbiato et al., 2009). It is a fundamental parameter used in the Rational Method (Eq. (1), a formula often used by hydrologists and engineers to calculate peak runoff due to its simplicity and widespread acceptance (Baiamonte, 2020; Chin, 2019; Dhakal et al., 2012). This method has been used in the analysis of drainage requirements and sizing of various hydraulic structures (e.g., storm sewer, culvert, pavement drainage, etc.) for small urban and rural catchments (Cleveland et al., 2011).

$$Q_P = kCiA \tag{1}$$

where k is the conversion factor (0.00278 for the given SI units of Q_P, i, A), Q_P = peak runoff (m^3/s), C = runoff coefficient (−), i = rainfall intensity (mm/h), and A = catchment area (ha). Within the rational method, the runoff coefficient, representing the integrated effects of catchment conditions, soil, and land use/land cover, is the most challenging to accurately determine. Namely, its estimation relies on the judgment of the engineers, as well as, through consultation with experts (Dhakal et al., 2012; Grimaldi & Petroselli, 2015). The main limitation of the formula stems from the use of typical C values derived from look-up tables found in hydrology textbooks and design manuals, which were developed with little basis on observed rainfall and runoff data (Dhakal et al., 2012; Young et al., 2009).

When rainfall and runoff data are available, the runoff coefficients of the given location can be obtained either by (a) inverting Eq. (1) and calculate C from the equation; or (b) volumetric approach, where C is the ratio of runoff volume to rainfall volume. In this study, the volumetric approach was employed to determine the event runoff coefficients of both studied catchments, as the ratio of event runoff (mm) over total event rainfall (mm), i.e., the fraction of rainfall amount that becomes runoff during or immediately following a rainfall event. These series of computed C from individual rainfall-runoff events were then used to obtain the mean and median C for each catchment and compared to the table of C values from ASCE manuals (ASCE, 1992; 1996).

3.2.2. Curve number

The curve number method is used to quantify runoff from individual rainfall events at the catchment scale and was developed by the United States Department of Agriculture Soil Conservation Service (USDA-SCS), now known as the Natural Resources Conservation Service (NRCS), mainly for small agricultural catchments (Banasik et al., 2014; Boughton, 1989; Hawkins et al., 2008; Soulis et al., 2009; USDA-NRCS, 2004; USDA, 1986; Wilson et al., 2017; Woodward et al., 2006) and subsequently updated to forested and urban catchments (Hawkins et al., 2008). This method estimates runoff (Q, mm) as a function of rainfall depth (P, mm), maximum potential retention (S, mm), and initial abstraction ($I_a = \lambda S$, where $\lambda = 0.2$) as defined in Eq. (2).

$$Q = \frac{(P - I_a)^2}{(P - I_a) + S} \text{ for } P > I_a \tag{2}$$

$Q = 0$ for $P \leq I_a$.

The parameter S (for SI units, mm) is mapped onto a dimensionless curve number (CN) as:

$$S = 25.4\left(\frac{1000}{CN} - 10\right) \tag{3}$$

that ranges from CN = 0, representing a theoretical upper bound to potential maximum retention ($S \rightarrow \infty$) with no direct runoff generated from a rainfall event to CN = 100 when a condition of zero potential maximum retention ($S = 0$) and all rainfall becomes a runoff. In most of the hydrological applications, CN values are typically selected from look-up tables found in design manuals and published handbooks, such as the USDA NRCS National Engineering Handbook (NEH) (USDA-NRCS, 2004) or Technical Release 55 (TR-55) (USDA, 1986), based on the hydrologic soil group, land use/land cover, and hydrologic conditions of the catchment. However, despite being a widely used and accepted method in hydrology, it is faced with a common difficulty, which is the use of tabulated CN values for local-level applications. Empirical evidence shows that CN can vary due to the dynamic nature of rainfall characteristics, seasonal changes in vegetation, and landscape differences (Ibrahim et al., 2022; Gonzalez et al., 2015; Lian et al., 2020; Muche et al., 2019; Singh & Mishra, 2019). Hence, the preference of estimating the CN parameter from local catchment data based on rainfall-runoff events has been a continuing topic of discussion among the (urban) hydrological science community.

Hence, where data from hydrometric and meteorological measurements are available, the value of S for $\lambda = 0.2$ was estimated from Eq. (4) after some algebraic calculations as described by Hawkins (1993). By substitution, event CNs were then calculated using Eq. (5).

$$S = 5\left[P + 2Q - \left(4Q^2 + 5PQ\right)^{1/2}\right] \tag{4}$$

$$CN = \frac{25400}{254 + S} \tag{5}$$

However, even when the CN is determined from measured P-Q data, the CN values calculated with Eq. (5) vary significantly from storm to storm on any catchment. For this reason, to estimate a single CN value describing the catchment in terms of measured runoff data, the central tendency (mean and median) and asymptotic fitting methods were used. The mean and median CN values were obtained from a series of event-based CNs, calculated using Eq. (4) and (5) for individual rainfall-runoff events of each catchment. These central tendency measures are frequently used as single CN values representing the characteristics of the catchment. In particular, the table of CN values stipulated in NEH (USDA-NRCS, 2004) used the median value of CNs from rainfall-runoff events. For the asymptotic fitting method, the measured rainfall and runoff data for each catchment were sorted separately and realigned on a rank order basis to form rainfall-runoff pairs having the same frequency of occurrence to compute corresponding CN, following the frequency matching technique (Hawkins, 1993; Hjelmfelt, 1980). The asymptotic fitting was also implemented using the natural sorting of data, where the runoff is matched with the rainfall event that caused it. By plotting the event CN against the causative rainfall, Hawkins (1993) identified three different behaviors, namely standard, complacent, and violent. In this study, the CN of both catchments was defined in standard behavior using the asymptotic equation (Eq. (6) recommended by Hawkins (1993).

$$CN(P) = CN_\infty + (100 - CN_\infty) \bullet \exp\left(-\frac{P}{b}\right) \tag{6}$$

where CN_∞ is the asymptotic constant CN approached as rainfall, $P \rightarrow \infty$ and to be taken as the representative CN of the catchment, b is the fitting parameter that describes the $CN(P)$ approaching the asymptotic constant CN_∞. Detailed descriptions of this method can be found in the publication of Hawkins (1993). The estimated CNs from central tendency measures and standard asymptotic fitting method were then compared to the tabulated CN values from USDA-NRCS (2004) and USDA (1986) and gridded values from GCN250 (Jaafar et al., 2019) based on average antecedent soil moisture condition (AMC II).

3.3. Statistical analysis

In order to differentiate the rainfall events according to their characteristics, they were clustered using a hierarchical clustering algorithm (Ward's minimum variance method on a distance matrix calculated by the Euclidean distance measure) (Zaki & Meira, 2014), based on the precipitation sum [mm], rainfall duration [h], and mean event intensity [mm/h]. Hierarchical clustering is a method that assigns cases based on

their similarity to clusters in order to create a hierarchy of clusters (Zabret et al., 2018). Grouping and splitting of the clusters is based on the measure of dissimilarity between sets of observations. The hierarchical clustering was carried out using the Orange software (Demšar et al., 2013). The degree of relationship between the considered variables was investigated using regression analysis with their statistical significance being assessed by one-way analysis of variance (ANOVA) at 0.05. Additionally, the estimated runoff coefficients and curve numbers in the urban mixed forest and urban area, as well as, for the growing and dormant seasons were compared statistically using a non-parametric Mann–Whitney *U* test at a 0.05 significance level.

3.4. Auxiliary analysis: Diurnal cycle of streamflow in the urban mixed forest

To gain a better understanding of the eco-hydrological processes in the urban mixed forest catchment and its dynamic response to environmental drivers, we investigated the diurnal pattern of streamflow in this catchment and the meteorological forcing that caused it. We focused on identifying the trends and dynamics of streamflow, evapotranspiration, and the streamwater viscosity where their diurnal trends were evaluated in an hourly resolution. The analysis utilized potential evapotranspiration (PET), which was obtained through the (air) temperature-based model developed by Oudin et al. (2005). The estimation of hourly PET was carried out in R software using the PE_Oudin function inside the airGR package (Coron et al., 2023). Conversely, the viscosity of the stream was determined based on the water temperature (in Kelvin, 5-minute resolution), following the Vogel equation as outlined by Schwab et al. (2016). Air temperature data was obtained from the meteorological station at the study site maintained and operated by the Slovenian Forestry Institute (Gozdarski inštitut Slovenije) while water temperature data was measured by the HOBO logger (Section 2.2). The present study employed a simple descriptive characterization of the diurnal patterns observed from the time series data of the variables. The seasonal structure of the diurnal amplitude, timing to maxima and minima, and shape of the diurnal cycle were analyzed for the variables of interest.

4. Results and discussions

4.1. Monitored rainfall-runoff events

The analyzed 86 rainfall events from August 2021 to August 2023 delivered a total rainfall amount of 2653 mm, corresponding to an average of 1326.5 mm per year. During the investigated period, a winter-spring precipitation deficit was observed in the greater Ljubljana area at the beginning of 2022, with only 266 mm of rainfall recorded between January and May 2022 (ARSO, 2022). This amount is 57 % lower than the long-term (1970–2021) average for the same 5-month period (ARSO, 2023). The dry period persisted until the summer of 2022 when a series of heatwaves caused extreme drought across Europe (Toreti et al., 2022). Fig. 3 illustrates the inter-annual variability of rainfall volume, duration, and mean intensity of all considered rainfall events, which are grouped into bimonthly classes. The 50th percentile rainfall event was found to be 21 mm, while storms $\leq$ 37.5 mm represent 75 % of observed rainfall events. Event mean rainfall intensities are defined as the ratio of cumulative rainfall amount over the storm duration. Moreover, 8 storm events registered an accumulated rainfall amount greater than the 90th percentile (63.18 mm), with 2 of those exceeding 100 mm (131.2 mm in August 2023 and 295.8 mm in September 2022), which were excluded in the boxplot. Hence, it can be observed from Fig. 3 that the rainfall amount exhibits seasonal variation, with the largest amount of rain occurring in autumn. Whereas rainfall duration is longer in wet and moderately wet seasons and significantly shorter in summer. More intense storm events occurred in the summer, specifically between June and August, compared to the wet periods.

Furthermore, the result of the hierarchical clustering led to the differentiation of rainfall events into 4 major groups as shown in the informative heatmap (Fig. 4) and boxplot (Fig. 5):

G1: Low rainfall amount, short duration, and low intensity (n = 51).

G2: High rainfall amount, long duration, low intensity (n = 18).

G3: Low to moderate rainfall amount, short duration, high intensity (n = 14).

G4: Moderate rainfall amount, short duration, very high intensity (n = 2).

More than half of the events analyzed are classified as G1, but in terms of rainfall sum per group, G2, consisting of long-duration heavy rainfall events, contributes 39 % to the total rainfall amount of the monitored storm events. Rainfall events with recorded consequences (i.e., flooding) are distributed in groups G2, G3, and G4, each of which features either a high volume of precipitation or a high-intensity rainfall. Thus, it is important to note that the statistics of G4 are associated with a significant degree of uncertainty given that only 2 events belong to this group. The same issue applies to G5, with only 1 event, which for this reason was not included as one of the rainfall groups. This particular event occurred on September 15, 2022 and delivered 295.8 mm of rainfall, which is the maximum rainfall amount during the study period and lasted for 58 h (> 250-year return period). Meanwhile, the most intense storm event occurred on July 5, 2022, with an average rainfall intensity of 49.9 mm/h (46.6 mm in less than an hour) and a return period of 20-year.

On the other hand, the results of the linear regression analysis

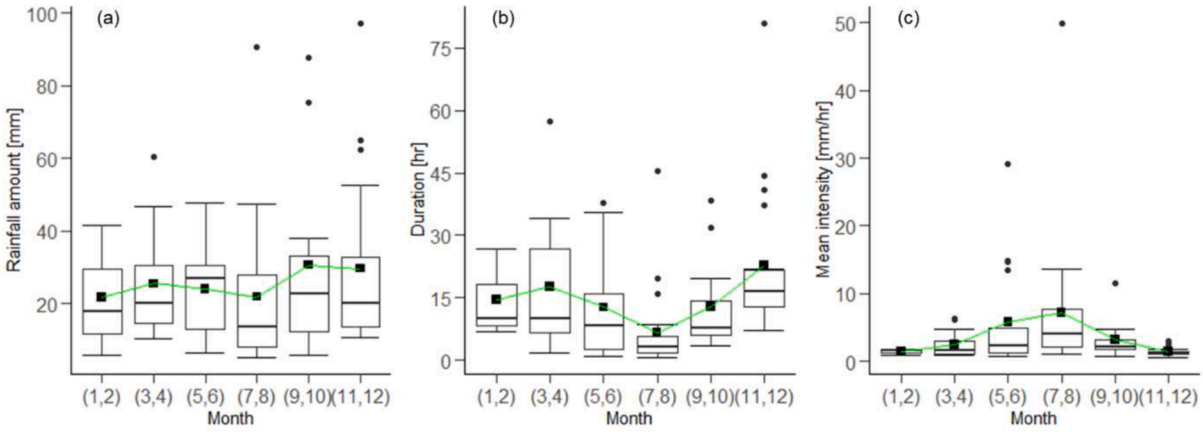

Fig. 3. Seasonal (bi-monthly) variability of rainfall characteristics in the period August 2021-August 2023: (a) rainfall amount; (b) rainfall duration; (c) mean rainfall intensity. Filled squares in the boxplot show the mean values.

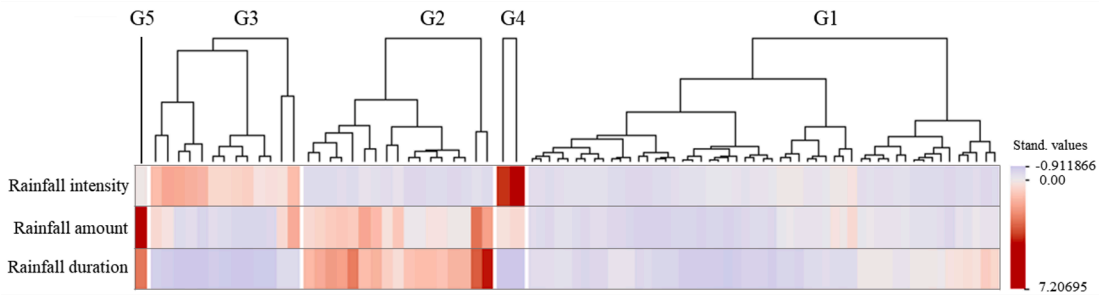

Fig. 4. Heatmap and hierarchical clustering of the standardized values of rainfall variables from 86 monitored storm events. The dendogram on the top was created based on Ward's method on a distance matrix calculated by the Euclidean distance measure.

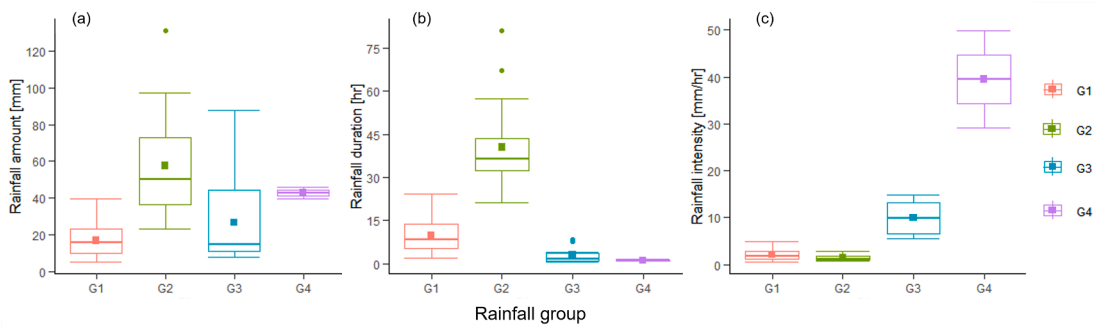

Fig. 5. Characteristics of the four rainfall groups (G1, G2, G3, G4) in terms of (a) rainfall amount; (b) rainfall duration; (c) mean rainfall intensity. Filled squares in the boxplot show the mean values.

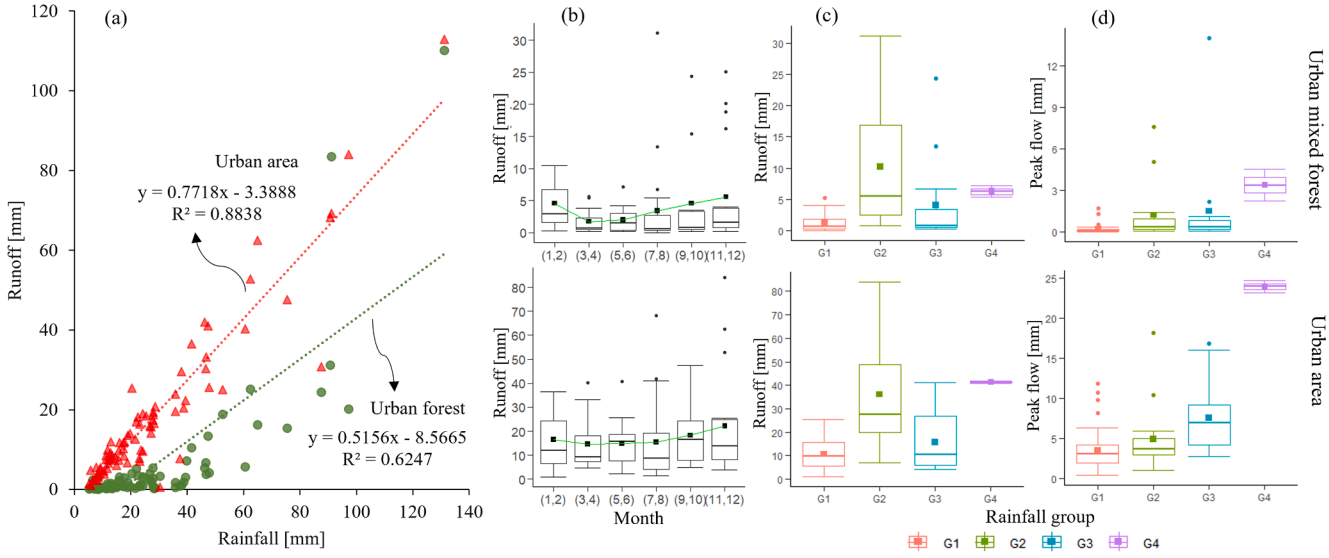

Fig. 6. Event rainfall–runoff relationship (a), seasonal (bi-monthly) variability of runoff (b), runoff volumes (c) and peak flows (d) per rainfall groups (G1, G2, G3, G4) in the urban mixed forest and urban area. Filled squares in the boxplot show the mean values.

(Fig. 6a) revealed a significant direct relationship between rainfall and runoff in both catchments: urban mixed forest ($R^2 = 0.62$; $p < 0.001$) and urban area ($R^2 = 0.88$; $p < 0.001$). This linear relationship aligns with the similar patterns we can observe from the boxplots of rainfall amount and catchment's runoff volume within the groups as shown in Fig. 5a and Fig. 6c, respectively. As expected, a greater proportion of rainfall in the urban area contributes directly to runoff generation, leading to higher runoff volumes (Fig. 6c) and peak flows (Fig. 6d) compared to the urban mixed forest. In fact, the ratio of the regression slopes between the urban area and urban mixed forest is 1.5, indicating that the urban catchment tends to produce an order of magnitude more runoff per unit of rainfall than the urban forest. This finding corroborates the well-established understanding that the presence of impervious surfaces remarkably enhances runoff generation compared to vegetated/forested areas. In addition, the higher variation of 88 % in runoff in the urban area catchment suggests that the influence of rainfall on runoff is even more pronounced in this setting compared to the urban mixed forest. While rainfall patterns show seasonal variations (Fig. 3), the response of both catchments in terms of runoff generation does not vary much seasonally (Fig. 6b) but autumn and winter rainfall events

were found to contribute the largest runoff volume.

Additionally, the boxplots in Fig. 6c and 6d visually represent the distribution of runoff volumes and peak flow within rainfall groups in both catchments. Regardless of the catchment, the highest runoff volumes originate from G2, which is characterized by long-duration heavy rainfall events, the characteristics of autumn–winter rainfall events in Slovenia (Kobold & Sušelj, 2004). It is also indicated in the boxplots that peak flow increases as rainfall events become more intense and have higher volumes, with a consistent increase in mean values from G1 to G4. The highest mean peak flow is observed in G4, reflecting the substantial impact of extremely high-intensity storm events on the runoff response of both catchments, particularly in the urban area. These observed disparities can be attributed to the contrasting land use/land cover and slope of both catchments. Unlike the urban area, where impervious areas create conditions that promote runoff generation, the vegetation (e.g., trees, shrubs) canopies and soil in an urban mixed forest can intercept and absorb a significant portion of rainfall, thus reducing both the quantity and rate of runoff.

4.2. Event runoff coefficients and curve numbers from measured rainfall-runoff data

The observed C values in the urban mixed forest were highly variable (CV > 1.0) and right-skewed (3.45), varying from 0.001 for a rainfall of 8.4 mm to 0.91 for a 91.2 mm rainfall, with a mean of 0.11 ± 0.016 (Table 1, Fig. 7a). More than half of the C values from the events are less than the mean and are clustered around the lower median C of 0.062. This distribution implies that using the mean C as the single representative value may overestimate the runoff generation in the urban mixed forest. The median, being less influenced by extreme values, offers a more stable and representative estimate of the C value. However, the use of the median C would also underestimate the runoff for extreme events, which can be particularly critical when designing infrastructure for flood protection. These events, although infrequent, can have significant impacts on the urban hydrological cycle and are important to consider in hydrological modelling and planning.

In contrast, the urban area consistently exhibited a significantly higher event C ($p < 0.001$), ranging from 0.17 to 0.96, with a more symmetric data distribution. Both the mean and median C values are estimated at 0.60, which are approximately 5 and 10 times higher than those observed in the urban mixed forest, respectively. Most of the C values observed in the urban area are clustered around the central tendency, indicating less variability across rainfall events. This likely reflects the dominance of impervious surfaces on the catchment's runoff behavior. In this case, the use of central tendency measures as the single lumped value of C may provide a reasonable representation of this specific catchment.

The estimated mean C values from the observed data fall within the range of tabulated C values reported in the design manual of the American Society of Civil Engineers (ASCE, 1992, 1996) for the specific land uses that closely resemble the dominant land uses in both studied catchments. According to these tabulated values, the C for parks (the closest land use to urban mixed forest) is between 0.10 and 0.25, while that for business or commercial neighborhoods (the closest land use to the studied urban area) ranges between 0.50 and 0.70. Within this range of C, McCuen (2005) recommended a C value of 0.20 for parks and 0.60 for business neighborhoods. However, when we refer to the table of runoff coefficient values as a function of the hydrologic soil group (A, B, C, D) and catchment slope, the forest is assigned a runoff coefficient of 0.20 to 0.25 for a hydrologic soil group D and a slope of greater than 6 %, which describes the soil and catchment characteristics of the urban mixed forest (average slope of 38.3 %). In this case, the computed mean event runoff coefficient of 0.11 is approximately two times lower than the tabulated C value for its characteristics. As for the studied urban area, the catchment is rather flat with an average slope of 7.1 % and a typical urban soil with anthropogenic admixtures (e.g., brick particles, concrete debris). Based on these attributes, the tabulated values assigned a runoff coefficient of 0.72 to 0.90 to commercial land use, from which the values demonstrate only minor variations between soil groups and slope range compared to other land uses.

As depicted in Fig. 7b, the linear relationship between rainfall and C is statistically significant in both catchments ($p < 0.001$), but the strength of the correlation is much stronger in the urban mixed forest ($R^2 = 0.56$) compared to the urban area ($R^2 = 0.14$). It implies that approximately 56 % of the variation in the C of the urban mixed forest and 14 % for the urban area can be explained by the variation in rainfall. However, as can be seen from Fig. 7b, the increase in C with rainfall amount was subjected to some dispersion. For example, in the urban mixed forest, similar C values of around 0.022 were observed for rainfall amounts of 8.6 mm and 37.4 mm occurring in different hydrological years of the study period. Also, rainfall events of 13 mm and 46.2 mm resulted in a comparable C of approximately 0.12. Whereas the C in the urban area remained consistently high, but certain rainfall events of varying amounts generated the same C, such as a C of 0.35 was observed for both 11.8 mm and 87.6 mm of rainfall, as well as 0.66 for 11.2 mm and 60.6 mm of rainfall, among others. Nevertheless, the analysis suggests that the volume of precipitation has a predictive role in determining the runoff coefficient for the outlet of the urban mixed forest catchment. This finding is consistent with the research conducted by Blume et al. (2007), which reported an increase in runoff coefficients in response to total precipitation. However, the lack of a strong association between rainfall and runoff coefficient suggests the relative influence and contributions of other factors that modulate the runoff generation processes, as also observed by Rodríguez-Blanco et al. (2012). This is particularly relevant in an urban area where different land uses/land covers have varying runoff mechanisms, implying the non-linearity of the rainfall-runoff processes in urban catchments.

In terms of CN, the central tendency measures from both catchments are less disparate and the distribution is more symmetrical (Table 1, Fig. 8a). Over the analyzed events, the average CN in urban mixed forest was 82.69 ± 0.919, ranging from 63.6 to 97.44, with a median CN of 83.95. As for the urban area, the mean and median CN are also considerably high at 95.45 ± 0.446 and 96.81, respectively, which varies from 74.1 to 99.65. Hence, using either the mean or median as a single representative CN value may provide a reasonable estimation of the studied catchment's hydrological behavior.

Additionally, an asymptotic fitting method proposed by Hawkins (1993) was applied to the naturally sorted and rank-ordered rainfall-runoff data pairs from both catchments. Fig. 8b and c illustrate the relationships between rainfall and observed CN for each catchment under natural sorting and rank-ordering of data pairs, respectively. These associations are described by exponential equations, as reflected in Fig. 8b and 8c, which is a projection of the standard asymptote indicated in the study by Hawkins (1993). It can be inferred from this analysis that both

Table 1
Summary of the descriptive statistics of runoff coefficients (RC) and curve numbers (CN) over all analyzed storm events.

Statistics	Catchment			
	Urban mixed forest		Urban area	
	C	CN	C	CN
Mean ± S.E.	0.11 ± 0.016	82.69 ± 0.919	0.60 ± 0.020	95.45 ± 0.446
Median	0.062	83.95	0.60	96.81
Std. deviation	0.15	8.11	0.18	3.94
Skewness ± S. E.	3.45 ± 0.261	−0.66 ± 0.272	−0.16 ± 0.267	−2.93 ± 0.272
CV	1.36	0.098	0.30	0.041
Asymptotic	–	71.71*	–	90.69*

S.E. – standard error; CV – coefficient of variation

* Asymptotic CN based on standard behavior under rank-ordered rainfall-runoff data pairs.

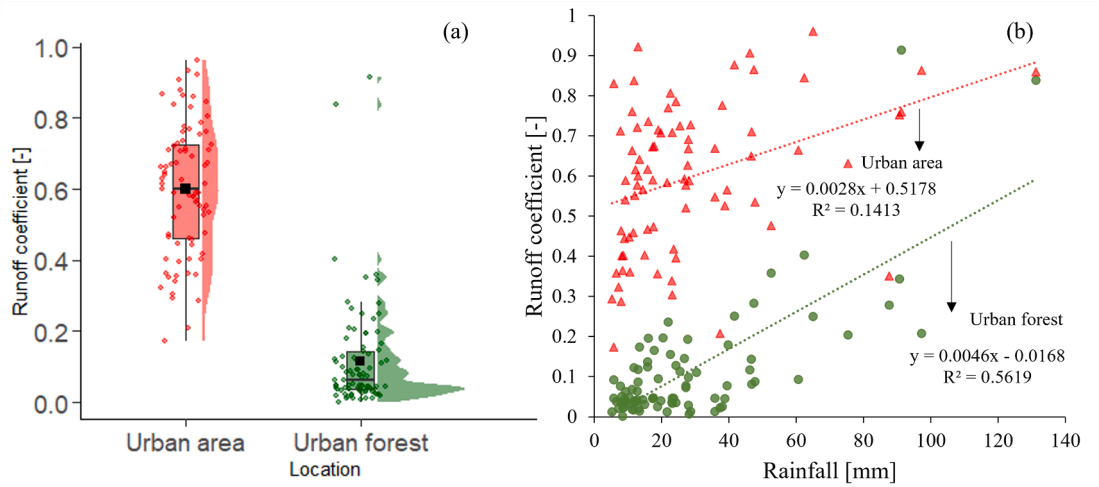

Fig. 7. Boxplot comparison of runoff coefficient (a); linear relationship between rainfall and runoff coefficient (b) from both locations across all monitored storm events. Filled squares in the boxplot show the mean values.

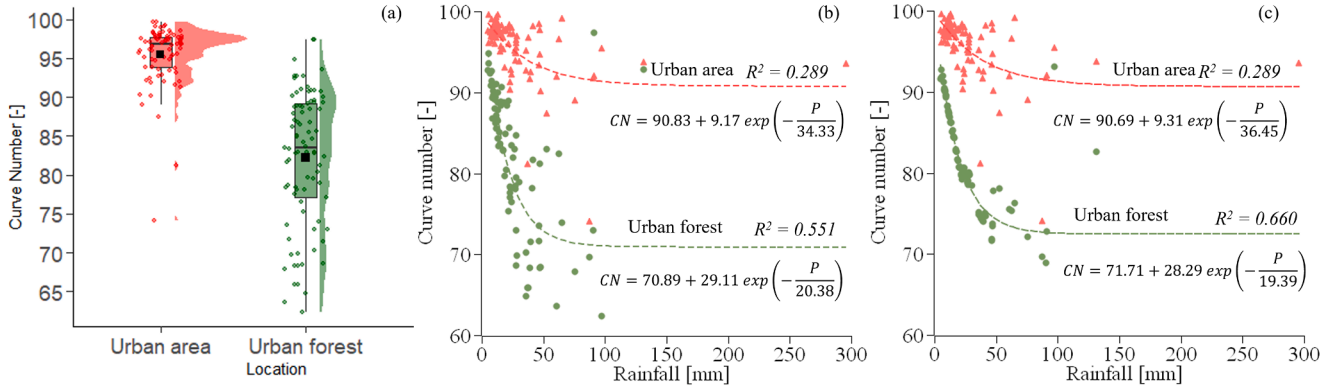

Fig. 8. Boxplot comparison of curve number (a); relationship between rainfall and curve number using natural sorting (b) and rank-ordered sorting (c) of observed rainfall-runoff data, with the approximation of standard asymptotic functions CN(P) using Eq. (6). Filled squares in the boxplot show the mean values.

catchments exhibited a standard behavior response, where the observed CN values decline progressively with increasing rainfall depth, approaching a stable near-constant CN value at larger storm events. This asymptotic CN (CN_∞) value is assumed to be the CN representative that characterizes the catchment (Hawkins, 1993). Certainly, Van Mullem et al. (2002) identified standard behavior as the most common scenario because Hawkins (1993) found that 70 % of the 37 studied small catchments showed this pattern. Recent studies have further supported this finding, reporting similar observations in their respective catchments. For instance, D'Asaro and Grillone (2012) observed a standard response in 43 out of the 61 catchments in Sicily; Banasik and Woodward (2010) found this type of behavior in a small agricultural catchment in Poland; Soulis (2018) identified the same response in the post-fire period of a small-scale experimental catchment in Attica, Greece; and Farran and Elfeki (2020) documented similar pattern in majority of the studied catchments in the southwest of Saudi Arabia. Hence, the natural sorting of data sets ($R^2 = 0.55$) from the urban mixed forest presents a greater dispersion of values around the regression line of the standard behavior compared to the rank-ordered series ($R^2 = 0.66$), as also observed in other studies (e.g., Farran & Elfeki, 2020; Strapazan et al., 2023). Nonetheless, a statistically significant relationship was found between rainfall and CN ($p < 0.001$) based on the relatively high coefficient of determination, further confirming the standard response of the catchment. Conversely, the urban area catchment exhibits a greater dispersion of values in both sorting techniques, accompanied by a less pronounced yet statistically significant association of CN with rainfall ($R^2 = 0.29$). For the purpose of facilitating a consistent comparison of CN with the tabulated values and prior estimates from central tendency measures, the asymptotic CN derived from rank-ordered data pairs will be used in the subsequent discussions.

As it appears from Fig. 8b and c, there is a clear tendency for CN to approach a stable asymptotic value at larger storm sizes in both catchments. These asymptotic CN (CN_∞) values correspond to 71.71 ± 1.356 for the urban mixed forest and 90.69 ± 1.632 for the urban area. In both cases, the CN_∞ values are lower than the CN derived from central tendency measures (i.e., mean and median). As expected, the observed CN values of the urban area are consistently higher than that of the urban mixed forest in both central tendency measures and asymptotic method. The combination of factors related to impervious surfaces, soil compaction, reduced vegetation, and land use heterogeneity contribute to a more runoff-prone environment in the urban area, leading to higher CN values and greater potential for surface runoff. Within the framework of NRCS NEH (USDA-NRCS, 2004) or TR-55 (USDA, 1986) documentation, an urban mixed forest does not have a direct land use/land cover equivalent, instead, the closest category would likely be woodland (some referred it as natural forests) cover type. Assuming a good hydrologic condition and average AMC II, the tabulated CN value for woodland ranges from 30 to 77, depending on the hydrologic soil group. On the other hand, the closest land use that can be associated with the studied urban area catchment is the commercial urban district with an

assigned CN of 89 to 95 across the various soil groups for AMC II. Thus, the reported mean and median CN values for the urban mixed forest are markedly higher than the range of CN provided by the NRCS. However, the estimated CN_∞ falls within the range of the tabulated CN, and considering the soil type D of the catchment, the CN_∞ value of 71.71 is lower compared to the NRCS-recommended CN of 77 for soil group D. As for the urban area, the estimated CN values based on central tendency and asymptotic methods are within the range of the reference CN values stipulated in NRCS documentation, consistent with the expected characteristics of the commercial-dominated urban area. Given the soil properties in this catchment, which vary between soil groups C and D, the mean CN (95.45) and median CN (96.81) values closely approximate the NRCS-tabulated CN of 94 and 95 for the respective soil groups. Whereas the CN_∞ of 90.69 is lower than the tabulated CN of NRCS. Previous related studies have also reported that the CN values based on the central tendency method are higher than the CN_∞ estimated from standard asymptotic fit and the NRCS NEH tabulated CN values (i.e., D'Asaro & Grillone, 2012; Oliveira et al., 2016; Singh & Mishra, 2019; Strapazan et al., 2023; Tedela et al., 2012a).

Furthermore, comparing the estimated CN to the values from the global gridded CN dataset (GCN250, Jaafar et al., 2019) reveals noticeable discrepancies. The GCN250 dataset aims to offer gridded, yet globally applicable, CN values at a 250 m spatial resolution based on global land cover (300 m), hydrologic soil group map (250 m), and a CN look-up table defining the different AMC levels (Jaafar et al., 2019). For the study location, GCN250 assigns a CN of 75 for the urban mixed forest and divides the urban area catchment into CN values of 88 and 91 under average antecedent conditions (Jaafar et al., 2019). The mean and median CN values for both catchments are higher than the reported values in the GCN250 dataset. Whereas, the asymptotic CN_∞ values obtained for both catchments are closer to the GCN250 values, suggesting that the gridded dataset may have captured the standard asymptotic behavior of CN in response to larger storm events. However, to substantiate this further, conducting additional local studies across different catchments is needed. The observed discrepancies can be attributed to the scale and resolution of the data, as our site-specific observations capture local conditions that the broader GCN250 dataset may have overlooked. Additionally, variations in land cover classification and hydrologic soil group definitions between our localized study and the global dataset can lead to discrepancies in CN assignment, as soil properties and land use can differ significantly even over small areas. Therefore, localized studies will benefit the GCN250 dataset as they can serve as an opportunity to further validate and refine the CN values in the GCN250 dataset with more site-specific hydrological data. This will subsequently improve the applicability and accuracy of GCN250 for use in localized hydrological modeling and stormwater management practices.

4.3. Seasonal variability of event-based runoff coefficients and curve numbers

Several studies have consistently demonstrated a distinct seasonality in runoff coefficients (i.e., Callegari et al., 2003; Merz & Blöschl, 2009; Rodríguez-Blanco et al., 2012) and curve numbers (D'Asaro & Grillone, 2012; Gonzalez et al., 2015; Muche et al., 2019; Strapazan et al., 2023; Tedela et al., 2007). On the other hand, Zheng et al. (2023) found that for highly urbanized catchments in Britain, less seasonality of event runoff coefficient was observed. In this study, the results of the Mann–Whitney *U* test revealed that the seasonal differences in the runoff coefficients and curve numbers between the growing and dormant seasons in both catchments were not statistically significant ($p > 0.05$). The lack of observed seasonal differences in curve number was also observed in some catchments in the United States of America with a humid subtropical climate (Tedela et al., 2007) and a humid continental climate (Tedela et al., 2012b). Van Mullem et al. (2002) further indicated that the seasonal variation of CN is less common in arid and semi-arid catchments but more prevalent in humid regions. Tedela et al. (2007) reasoned out that this observation could possibly be due to the inclusion of rainfall-runoff events occurring during the seasonal transition periods, which may possess similar characteristics of both growing and dormant seasons. In the context of our findings, one plausible explanation for the absence of statistically significant seasonal variations in C and CN in both catchments is that the number of rainfall events within the observation period may not have been sufficient to establish such statistically significant differences. With limited rainfall events, which may be partly attributed to the precipitation deficit at the start of 2022 and the subsequent summer drought, it becomes challenging to capture the full range of variability and identify meaningful seasonality patterns. Additionally, if there was high variability within each season, particularly when dealing with a limited number of rainfall events, it could obscure or overshadow any potential differences between the seasons. Another relevant contributing factor to this observation could be attributed to the rainfall partitioning of the urban mixed forest, as the study of Kermavnar and Vilhar (2017) indicated that throughfall (the fraction of rainfall that passes through the canopy and reaches the ground) in this mixed forest did not show statistically significant differences ($p > 0.05$) between the growing and dormant seasons.

In this case, inspecting C and CN on a bi-monthly basis may provide a more nuanced understanding of their variability. In terms of C, the months of September and October (autumn), during which most of the long-duration heavy rainfall events occurred (Fig. 3a) have the highest mean runoff coefficient for both catchments as shown in Fig. 9. It is followed by the months of November-February and July-August, which correspond to winter and summer, respectively. Similarly, Rodríguez-Blanco et al. (2012) observed a seasonal evolution in the runoff

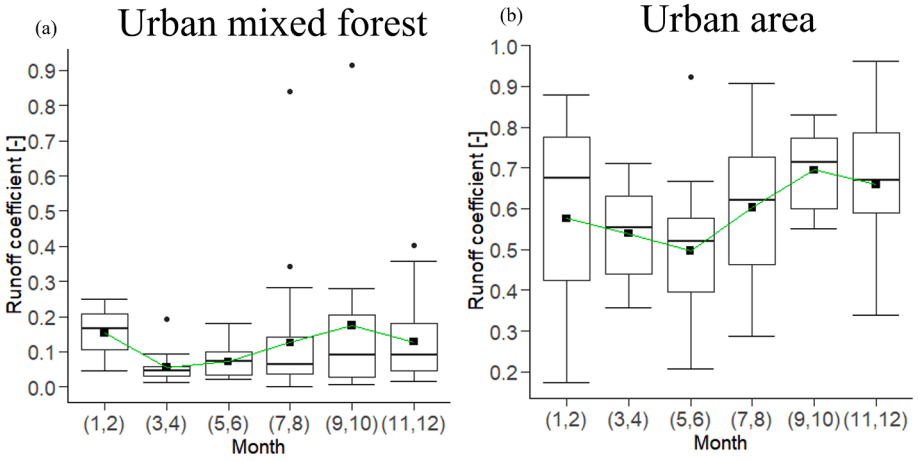

Fig. 9. Seasonal (bi-monthly) variability of runoff coefficient in the (a) urban mixed forest and (b) urban area.

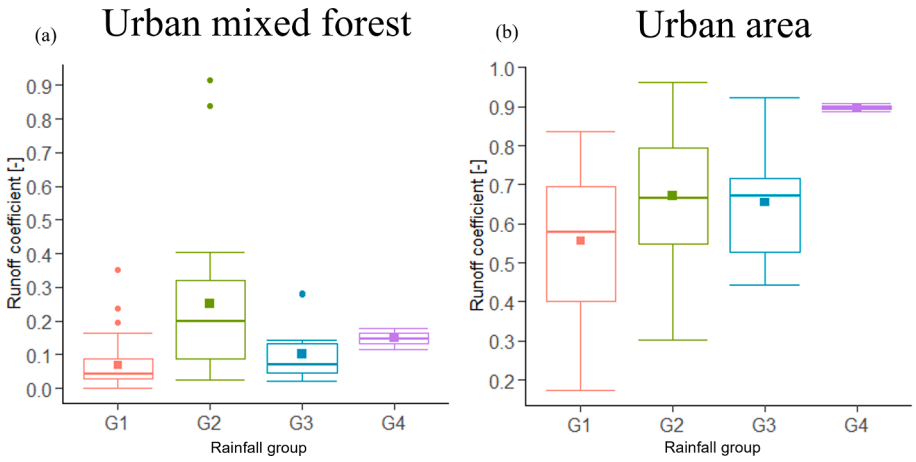

Fig. 10. Variability of runoff coefficient per rainfall groups (G1, G2, G3, G4) in the (a) urban mixed forest and (b) urban area.

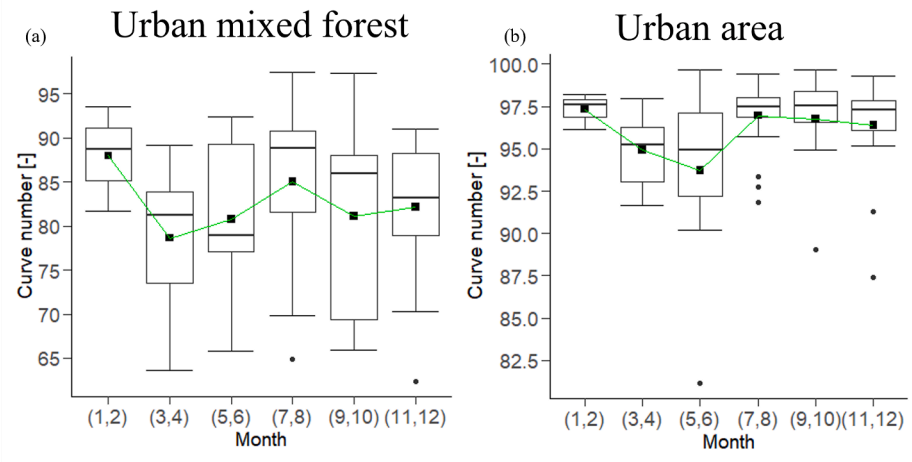

Fig. 11. Seasonal (bi-monthly) variability of curve number in the (a) urban mixed forest and (b) urban area.

coefficients of a forest-covered Corbeira catchment in Spain, with the highest values in autumn and winter, but with the lowest values occurring in summer. Birkinshaw et al. (2021) also observed that across most catchments in the UK, the highest runoff coefficient values were in winter (December-February) and the lowest values in summer (June-August), which coincides with the seasonal dynamics of evapotranspiration. The same observations were reported by Merz and Blöschl, 2009 for Austrian catchments except for the alpine region and by Callegari et al. (2003) for the Calabrian pine (*Pinus laricio* Poiret) forest stands in Italy, before and after thinning. Chen et al. (2020b) focused on the Hydrological Open-Air Laboratory (HOAL) in Austria and found that the largest runoff coefficients, with a median over 0.2, occurred in January/February, contrasting with a median below 0.035 in July to October. They further added that wetlands exhibited a less pronounced seasonal pattern, with runoff coefficients varying only slightly between months (median between 0.03 and 0.07).

As depicted in Fig. 11, a different trend can be observed in the bi-monthly variability of CN, particularly in the urban mixed forest. The months of January and February (winter), when soil moisture is high (in the urban mixed forest, Fig. 13), have the highest curve number in both catchments, followed by July and August (summer). Similarly, higher CN values were also observed during the growing season compared to the dormant season in all the catchments investigated in the United States of America (Tedela et al., 2007; Tedela et al., 2012b). In a semi-arid catchment in India, Gundalia and Dholakia (2014) highlighted the variability in CN values throughout the monsoon season, with the highest CNs observed in September and the lowest in October, consistent across the estimation methods used (i.e., median, geometric mean, and standard asymptotic fit). This seasonal variation aligns with the monsoon pattern, where September typically marks the peak of the monsoon with substantial rainfall while October represents the retreat of the monsoon, with significantly reduced rainfall. On the contrary, Gajbhiye et al. (2013) found that out of 4 evaluated catchments in a sub-tropical sub-humid region in India, 2 of those recorded a maximum curve number in June, and the other 2 had in July.

The pre-event soil moisture in the urban mixed forest for both in the open area of the catchment and under the forest canopies varies seasonally with drier months from July to October (Fig. 13). Notably, while most studies have reported the lowest C and CN during summer due to the drier soil conditions of the catchment (Merz & Blöschl, 2009), our analysis revealed that spring (March to May) exhibited the lowest values, which is also reflected in the amount of average runoff (Fig. 6b). Thus, it is important to acknowledge that the rainfall deficit in spring of 2022 may have influenced this observation. On the contrary, the plausible factor explaining the high C and CN during July and August could be related to the distribution of rainfall in the study location in which according to the long-term data (1970–2022) from the Ljubljana-Bežigrad meteorological station, summer is the 2nd wettest season, receiving 28 % of the annual rainfall, after autumn (31 %). Additionally, summer rainfall is often characterized by high-intensity events. The occurrence of these high-intensity storm events during summer and long-duration events in autumn can override the antecedent dry conditions of soil in

the urban mixed forest, because of the potential of these events to quickly saturate the soil and exceed its infiltration capacity. The study of Zabret et al. (2023) also highlighted the influence of rainfall intensity on soil moisture response in a small urban park in Ljubljana, Slovenia. It was observed that the soil moisture in the open area and below the open-grown trees increased rapidly in response to intense rainfall and the maximum soil moisture values were reached quickly (Zabret et al., 2023). Considering the soil type in the urban mixed forest as silty clay loam with a very low infiltration potential and the presence of impervious surfaces in the urban area catchment, it potentially caused more surface runoff and increased the runoff coefficient and curve number. Despite the urban mixed forest can intercept rainfall, such rainfall events can overwhelm the forest's interception mechanisms, especially when such events occur during the dormant season when the trees are in their leafless state. The findings of Zabret et al. (2023) further corroborate that during the leafless period, which typically corresponds to the wetter months of the year, the soil below the tree canopy responded more quickly to rainfall and even lower rainfall intensities induced a response to soil moisture. Moreover, the study by Chen et al. (2020a) highlighted the influence of precipitation characteristics, particularly duration, on predicting the runoff coefficient for the tile drainage and outlet systems. On the other hand, the urban area catchment, with its increased impervious surfaces and compacted soil properties, is more sensitive to high-intensity events, which is typical for urban areas (Agonafir et al., 2023; Marelle et al., 2020).

It can be seen in Fig. 10 that the distribution of runoff coefficients per rainfall group follows similar trends as the amount of rainfall (Fig. 5a) and runoff (Fig. 6c). Long-duration heavy rainfall events (G2) generated the largest mean runoff coefficient for the urban mixed forest, while extremely high-intensity events (G4) were responsible for the high runoff coefficients in the urban area. In contrast, the distribution and trend of the curve number (Fig. 12), in terms of mean and median, slightly deviates from this observed pattern with the rainfall group. For the urban mixed forest, the highest curve number is associated with rainfall group G3, characterized by moderate rainfall amount and high-intensity events. Unexpectedly, G4 recorded the lowest curve number in this catchment, but it is important to mention that this specific group only consists of two events, which therefore may not be sufficient to establish a definitive finding. Whereas the urban area exhibits its highest curve number with the G4 rainfall group, followed by G3, indicating a more expected response where heavier rainfall leads to more runoff due to the higher prevalence of impervious surfaces that inhibit infiltration. Hence, due to the statistical limitations (i.e., the limited number of events in certain rainfall groups), it is possible that the observed trend of CN with rainfall group is not representative of the overall pattern, and additional data encompassing more rainfall events, with extremely high intensity, across various seasonal conditions would be necessary to further validate these hypotheses. Also, the observed inconsistency and contradicting trends of runoff coefficients and curve numbers, particularly in the urban mixed forest likely reflect the different ways in which these two indices are calculated and the different factors that affect them.

4.4. *Specific single event analysis of runoff response and pre-event soil moisture conditions in the urban mixed forest*

In the present study, the relation of runoff coefficient and curve number with initial soil moisture is not as straightforward as expected. Previous studies have also indicated that the correlation between pre-event soil moisture and the subsequent runoff coefficient is relatively weak (i.e., Meißl et al., 2020; Penna et al., 2011; Uber et al., 2018). We have observed in Fig. 7b that certain rainfall events sharing similar characteristics can yield different Cs while events with distinct rainfall characteristics can exhibit similar Cs. These intriguing variations in catchment response observed in the urban mixed forest may be partially explained by the differences in pre-event soil moisture conditions. Hence, to better understand the interplay between rainfall, pre-event soil moisture, and the runoff response in the urban mixed, we analyzed specific rainfall-runoff events, as illustrated in Figs. 14-16. Events 27 and 73 (Fig. 14) were among the events with contrasting rainfall characteristics that have the same C of around 0.12. However, these events were characterized by distinct initial soil moisture conditions. The high-intensity event 27 occurred during the onset of the summer drought in July 2022 when the soil moisture was relatively low (< 25 % for the open area and < 18 % under the forest). In contrast, event 73 (June 13, 2023) was preceded by several independent (following the 4-h minimum inter-event time) moderate to heavy storm events, occurring between June 2 and 7, 2023, with rainfall amounts ranging from 13.2 mm ($C = 0.021$) to 40.6 mm ($C = 0.18$). It is hypothesized that the high C of event 73 despite the low rainfall volume can be due to high initial soil moisture and its high mean intensity (13.4 mm/h). The antecedent rainfall events effectively saturated the topmost 16 cm of the soil profile (both in the open and under the forest), creating favorable conditions for higher runoff potential. This pattern is further underscored by the corresponding CN values of 71.7 for event 27 and 90 for event 73, which highlights the significant influence of initial soil moisture on CN values. On the other hand, events 17 and 74 (Fig. 15) have almost identical rainfall characteristics but had differing Cs of 0.19 and 0.073, along with CNs of 84.7 and 78.1, respectively. These discrepancies can be explained by the initial soil moisture conditions before the occurrence of these events. Specifically, event 17 (27.8 mm) occurred during the beginning of spring, around 6 h after the first rainfall impulse of 38.8 mm ($C = 0.045$). This prior rainfall event notably increased the soil moisture content from 35 % to 39 % in the open area and from 26 % to 32 % under the forest, which served as the antecedent soil moisture condition for event 17, contributing to its

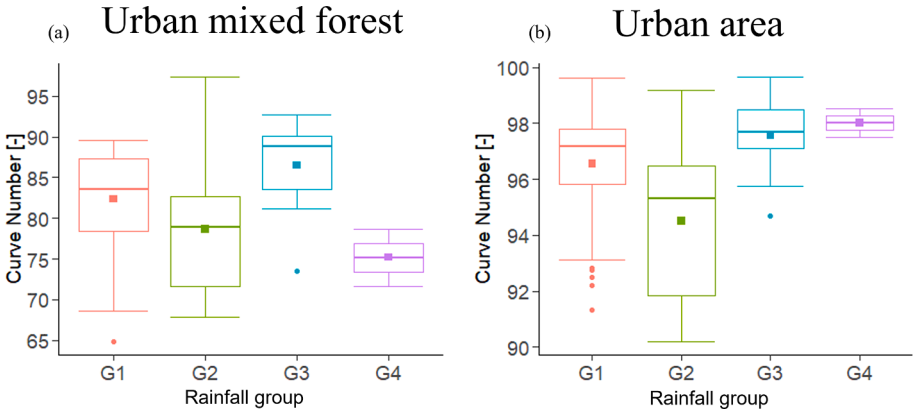

Fig. 12. Variability of curve number per rainfall groups (G1, G2, G3, G4) in the (a) urban mixed forest and (b) urban area.

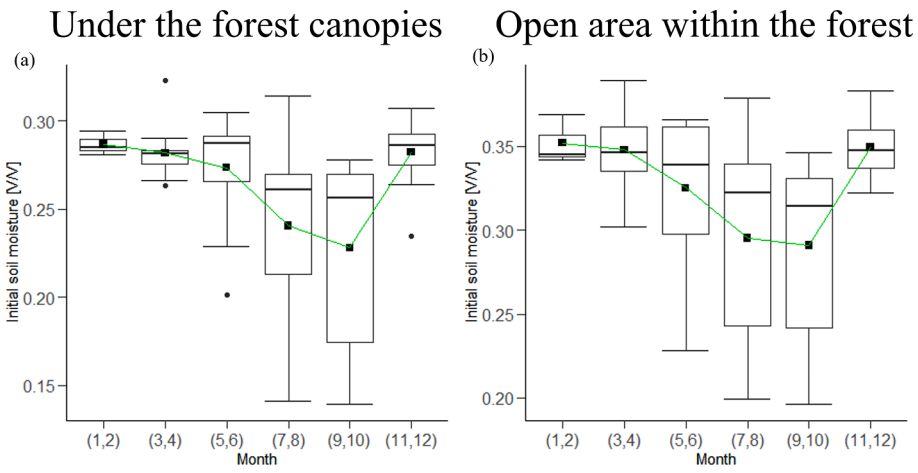

Fig. 13. Seasonal (bi-monthly) variability of pre-event soil moisture at 16 cm depth in the (a) open area and (b) under the forest canopies.

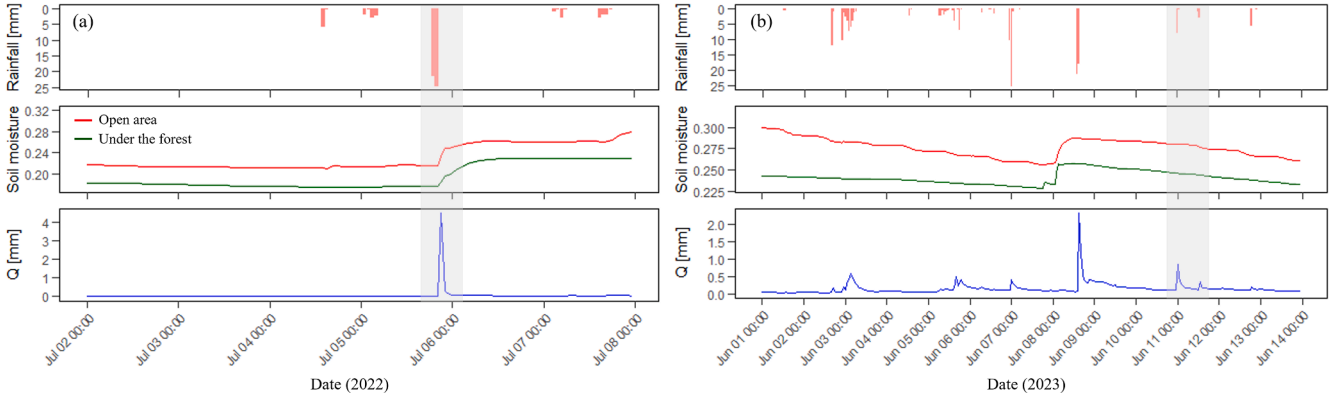

Fig. 14. Example of rainfall events with different characteristics but similar C and the subsequent response of upper soil moisture at 16 cm depth (in the open area and under the forest) and runoff. (a) Event 27 occurred on July 5, 2022 with a cumulative rainfall amount of 46.2 mm and mean intensity of 49.9 mm/h; (b) Event 73 occurred on June 11, 2023 with a cumulative rainfall amount of 13 mm and mean intensity of 13.4 mm/h.

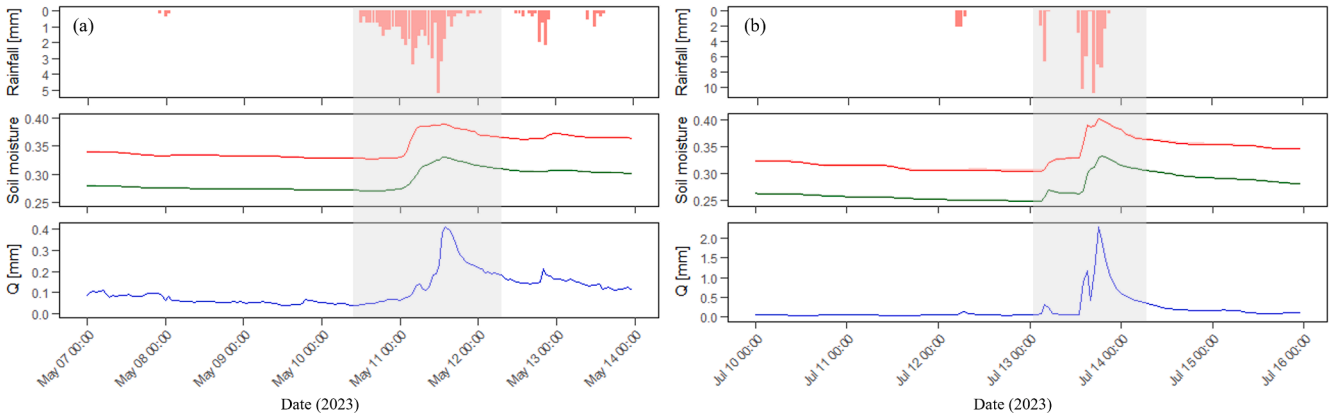

Fig. 15. Example of rainfall events with almost similar characteristics but different C and the subsequent response of upper soil moisture at 16 cm depth (in the open area and under the forest) and runoff. (a) Event 17 occurred on April 1–2, 2022 with a cumulative rainfall amount of 27.8 mm and mean intensity of 0.81 mm/h; (b) Event 74 occurred on June 27–28, 2023 with a cumulative rainfall amount of 27.2 mm and mean intensity of 13.4 mm/h.

higher C. The low C and CN of event 74 (27.2 mm) can be attributed to the drier conditions of soil with a pre-event moisture level of 28 % (open area) and the absence of precipitation within 10 days before its occurrence.

Further analysis of extremely heavy rainfall events (295.8 mm) following a prolonged dry soil condition at a moisture level of 22 % in the open area and 16 % under the forest (Fig. 16) due to the summer drought revealed that greater rainfall volumes do not necessarily equate to high C and CN. This particular storm event was characterized by a C of 0.26 and a CN of 39.3. However, this event effectively saturated the soil,

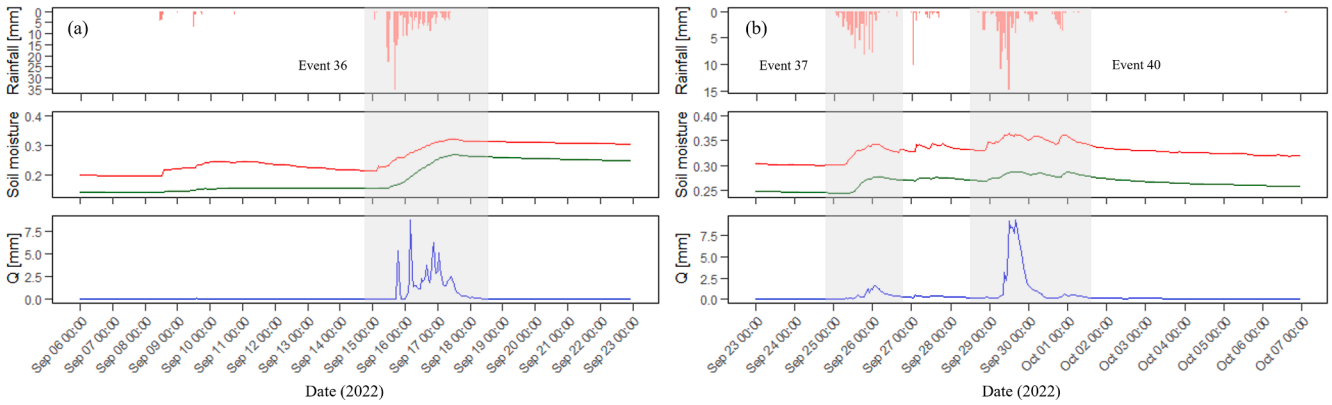

Fig. 16. Example of heavy rainfall events after a prolonged drought period and the subsequent response of upper soil moisture at 16 cm depth (in the open area and under the forest) and runoff. (a) Event 36 occurred on September 15–17, 2022 with a cumulative rainfall amount of 295.8 mm and mean intensity of 5.1 mm/h; (b) Event 37 occurred on September 25–26, 2022 with a cumulative rainfall amount of 75.4 mm and mean intensity of 2.0 mm/h, while event 40 occurred on September 28–30, 2022 with a cumulative rainfall amount of 91.2 mm and mean intensity of 2.7 mm/h.

reaching a constant moisture level of 32 % in the open and 25 % under the forest, setting the antecedent soil moisture condition for the next rainfall events. Event 37, which ensued 7 days after event 36 and featured a rainfall amount of 75.4 mm, occurred under these updated pre-event soil moisture conditions, and yielded an C of 0.20 and CN of 67.9. This event along with the occurrence of intermediate small rainfall events further increased the soil moisture to 34 % in the open and 27 % under the forest. This event along with the occurrence of intermediate small rainfall events further increased the soil moisture to 34 % in the open and 27 % under the forest. Such wet initial soil moisture conditions during the leaf-fall period of trees led event 40 with 91.2 mm of rainfall to have a significantly higher C of 0.91 and CN of 97.4. The elevated soil moisture levels and the preceding rainfall events contributed to this substantial increase in C and CN. The analysis of specific rainfall-runoff events demonstrates that pre-event soil moisture and/or antecedent rainfall can partly explain the dispersion of C in Fig. 7b and CN in Fig. 8 for the urban mixed forest.

4.5. *Diurnal streamflow pattern in the urban mixed forest*

Urban forests are among the green spaces found in urban environments with a multitude of ecosystem services, making them a valuable element of the green infrastructures in cities (Berland et al., 2017; Kong et al., 2021; Orta-Ortiz & Geneletti, 2022). Among the crucial benefits of urban forests is their role in urban stormwater management, which is especially significant given the increasing frequency of extreme weather

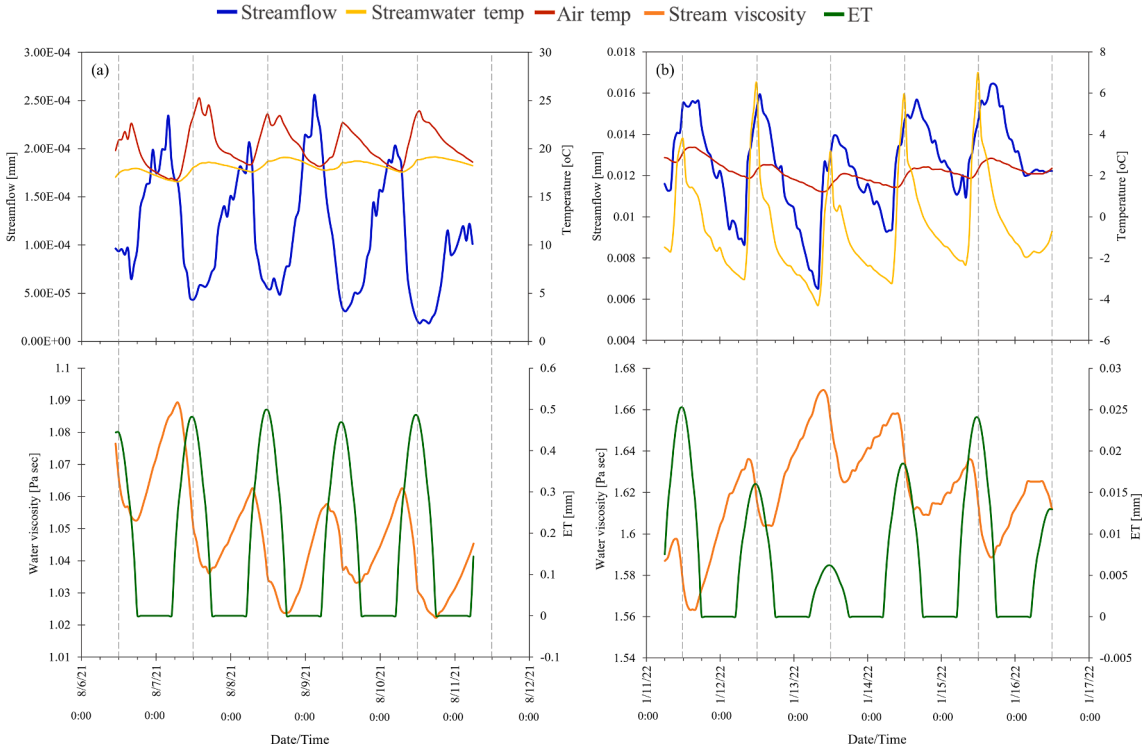

Fig. 17. Diurnal variations in streamflow, air/water temperatures, evapotranspiration, and streamwater viscosity during (a) winter – January and (b) summer – August. Hourly evapotranspiration was estimated using PE_Oudin function inside the airGR package (Coron et al., 2023) in R software, which uses the temperature-based formula from Oudin et al. (2005). Broken gray vertical lines in each plot indicate 12:00 noon (mid-day) and the minor tick in the x-axis is by 6-hr interval.

events due to climate change. They act as a natural sponge by increasing the hydrological losses in the catchment, mainly by canopy interception, evapotranspiration, and enhanced infiltration (Berland et al., 2017). Hence, understanding the eco-hydrological processes within urban forests is crucial for maximizing their functionality and benefits, particularly regarding stormwater management. Analyzing the diurnal variations in streamflow is a key part of this understanding as these patterns provide insights into how urban forests respond to the changes in environmental drivers and land cover (Deutscher et al. 2016).

The diurnal cycle in streamflow may be used as a diagnostic tool to identify the dominant processes affecting the water balance of a given catchment and thus, represents a significant part of the variability in streamflow observed in many rivers (Deutscher et al., 2016; Lundquist & Cayan, 2002; Schwab et al., 2016). Lundquist and Cayan (2002) outlined 4 mechanisms that induce diurnal patterns in streamflow, namely evapotranspiration, infiltration in losing reaches, diurnal cycles in rainfall, and snowmelt.

Visual inspection of the 2-year streamflow data in the urban mixed forest catchment indicated that the diurnal streamflow pattern is most prevalent during low flow and precipitation-free periods. Based on this time series, the catchment began to yield diurnal signals in streamflow in late spring and gradually developed a more clearly discernible signal amplitude during summer. These diurnal signals then became less pronounced during autumn, eventually being absent in winter, depending on the volume of rainfall received by the catchment during these periods. The characteristics of the diurnal cycle in streamflow also exhibit seasonal structures in terms of the shape and timing of maxima and minima (Fig. 17), as also described in other studies (i.e., Gribovszki et al., 2006; Lundquist & Cayan, 2002; Schwab et al., 2016). As an example, we selected a 6-day period in both summer (August 2021) and winter (January 2022) seasons when the diurnal cycles in streamflow were evident. This is also to demonstrate the interaction of the diurnal fluctuations between streamflow, evapotranspiration, and streamwater viscosity in both seasons. It can be observed from Fig. 17 that the summer diurnal cycle in streamflow is characterized by a gradual rise of about 14 h and a sharp decline of about 10 h. During this time, the hourly timing of the diurnal streamflow maxima occurred in the early morning, between 3:00 AM to 6:00 AM when both the air and streamwater temperatures were at their minimum. This corresponds to a period when the evapotranspiration rates of vegetation in the forest are typically at their lowest due to cooler temperatures and higher humidity. Simultaneously, lower water temperature tends to increase the streamwater viscosity, which can have a subtle effect on the hydraulic conductivity and infiltration rates of the streambed. This higher viscosity can impede the movement of water through the streambed material, reducing the infiltration rate (Bouwer, 2002; Miller et al., 2005; Ronan et al., 1998). Consequently, more water is available to contribute to streamflow in the channel. In contrast, the minimum streamflow during summer was observed in the afternoon (1:00 PM to 3:00 PM) when water and air temperatures were higher, causing a decrease in water viscosity and an increase in evapotranspiration, respectively. Lower viscosity allows the water to move more easily through the streambed material due to higher hydraulic conductivity, thus more water can infiltrate into the streambed (Constantz et al., 1994; Schwab et al., 2016). Thus, the combined effects of higher evapotranspiration and lower viscosity of water may explain the streamflow minima during this time of the day, but their relative contribution to the streamflow loss should be investigated more in detail in the future study. Conversely, when the diurnal streamflow pattern is present during winter (like in January 2022), it exhibits a steep rising limb that takes approximately 3 h, followed by a very gradual falling limb that lasts for about 21 h. The diurnal cycle reached the maximum streamflow in the afternoon, between 1:00 PM to 2:00 PM, during the dormant season when the viscosity is low and the minimum in the morning (9:00 AM to 10:00 AM). Based on this analysis, we hypothesized that the viscosity of streamwater has a potential relevant contribution to the observed diurnal cycle of streamflow in the urban mixed forest. The experiment of Constantz et al. (1994) concluded that the effect of stream temperature on the hydraulic conductivity of the streambed accounted for nearly all of the variation in streamflow loss. Also, they added that the maximum water loss observed in the afternoon caused the streamflow minima during this time. However, the study by Schwab et al. (2016) indicated that the diurnal streamflow maxima in the afternoon during the dormant season could be attributed to the viscosity effect of the inflowing water, while the minima in the afternoon during the growing season could be due to the greater relative significance of evapotranspiration. Nevertheless, recent studies at other catchments in different geographical locations further support that the diurnal pattern in streamflow can be potentially explained by the fluctuations in evapotranspiration and streamwater viscosity (Constantz et al., 2016; Schwab et al., 2016).

5. Limitations and future works

Both C and CN are typically used in lumped-parameter hydrological models, which cannot represent the spatial heterogeneity of the catchment characteristics, like distributed models do. However, distributed models require more data with higher spatial resolution which may not be available in many areas (Mishra et al., 2007; Strapazan et al., 2023). Hence, lumped models, particularly when informed by locally derived C and CN values, remain a valuable tool for hydrological modeling in data-limited environments, minimizing the uncertainty associated with parameter selection. However, during the estimation of C and CN from local gauged data, this study has several limitations that could serve as a springboard for further research.

The observation period covered in this study is relatively short, which is 2 years, and incorporating longer rainfall-runoff records is critical for capturing a more comprehensive range of hydrological conditions and temporal variations. It also ensures a more representative and statistically sound analysis, addressing potential biases or uncertainties that may arise from relying on limited datasets. These aspects are essential for more accurate estimations of the C and CN of both catchments, especially for the seasonality of both parameters, as well as for the calibration and validation of these estimated values.

The hydrograph baseflow separation for the urban mixed forest catchment was performed using the Lyne and Hollick (1979) recursive digital filtering method, which may affect the quantity of direct runoff. However, it is worth mentioning that the baseflow in this catchment constitutes a relatively small component of streamflow, with surface runoff being the dominant hydrological process. The catchment experiences rapid runoff during heavy rainfall events, when baseflow may be suppressed as water is quickly channeled away. This could be attributed to the catchment's steep slope (38.3 %) and the low infiltration capacity of the soil (silty clay loam). Nevertheless, it would be beneficial for further studies to compare several baseflow separation methods to better describe the hydrological processes of the catchment.

In calculating CN, we used a constant initial abstraction ratio, $\lambda = 0.2$, which has limitations that should be acknowledged. Previous research suggests that λ can vary depending on site-specific conditions and storm events (Hawkins et al., 2002; Mishra & Singh, 2004; Tedela et al., 2012a; Woodward et al., 2003). Also, we assumed an average antecedent moisture condition (AMC II) for the urban mixed forest catchment to facilitate comparison with the tabulated CN values. Future studies should investigate the actual AMC of the catchment and determine λ values by analyzing observed rainfall-runoff events, as well as explore the sensitivity of CN to different λ values to improve the accuracy of runoff estimates.

It is also imperative to test the runoff prediction performance of the estimated C and CN values from local rainfall-runoff data and compare them with the tabulated C/CN values, while also accounting for the seasonal variations of these parameters. Such research will help improve the accuracy and reliability of rational and curve number methods in hydrological analysis and engineering design, as well as the suitability

and limitations of using tabulated values in different hydrological contexts.

Urban environments exhibit a diverse range of land use patterns and are increasingly vulnerable to extreme weather events, highlighting the necessity for future studies that explore different urban land use types and climate change scenarios on C and CN. Such studies will aid in designing adaptive stormwater management strategies, contributing to more resilient urban infrastructures and cities. Enhanced empirical data and model predictions will also facilitate the implementation of nature-based solutions in cities and sustainable urban development practices globally.

6. Conclusions

C and CN are among the fundamental parameters in hydrology, crucial for understanding the hydrological responses to rainfall events at the catchment scale. In this study, we examined and compared the C and CN derived from observed rainfall-runoff events in the urban mixed forest and highly impervious urban area in Ljubljana, Slovenia. The results suggest that using central tendency measures as the single representative C values for the urban mixed forest is problematic due to high variability, while for the urban area, this method may provide a reasonable estimate of the catchment's runoff. These C values are lower compared to the tabulated C values specified in the design manual of the American Society of Civil Engineers for the respective land use. Conversely, the estimated mean and median CN values can be used as a representative single CN value to characterize the runoff potential of both studied catchments. The asymptotic CN_{∞} values for the urban mixed forest (71.71) and urban area (90.69) are lower than the NRCS NEH-tabulated values of 77 and 95, respectively, suggesting central tendency CN values to be higher than those from standard asymptotic fits and NRCS NEH tables.

Moreover, the bi-monthly analysis of event C and CN values showed distinct seasonal variations despite a lack of statistically significant differences between growing and dormant seasons. The C was highest during autumn and winter, particularly in September-October. In terms of CN, the months of January and February had the highest CN values, followed by July and August. The occurrence of high-intensity storms in the summer and prolonged heavy rainfall events in autumn may have overridden the dry antecedent soil conditions, resulting in increased C and CN values. Event analyses revealed that pre-event soil moisture and antecedent rainfall caused some rainfall events with different characteristics to have similar C, while events sharing the same characteristics have different C. The interplay of pre-event soil moisture conditions, antecedent rainfall events, and the characteristics of specific storms significantly influenced the observed variations in C and CN, thus shaping the runoff response.

By demonstrating the discrepancies between the estimated values of C/CN from local gauged data and the generalized tabulated values, this study challenges the conventional use of generic hydrological parameters and underscores the necessity for site-specific estimates of these parameters based on gauged data. Reliance on generalized tabulated values may lead to underestimations or overestimations of runoff, impacting the design and efficacy of urban drainage systems and stormwater management strategies. Additionally, given the observed seasonal variations in C and CN, it is crucial to factor in temporal changes when designing stormwater management systems. The findings highlight an opportunity for municipalities to re-evaluate and potentially revise the design guidelines of their urban water infrastructures to better reflect local conditions. However, caution is still advised when interpreting and using the estimated values from this study in hydrological analysis and design of hydraulic structures, particularly for the study location.

In addition to this, the diurnal streamflow pattern in the urban mixed forest catchment showed distinct seasonal characteristics, in terms of the diurnal shape and the timing of streamflow maxima and minima. The diurnal cycle in streamflow is more prevalent during low-flow and precipitation-free periods. The understanding of this component of the eco-hydrological processes is crucial for optimizing the functioning and benefits of urban forests as one of the nature-based solutions for climate change adaptation and sustainable development.

In summary, site-specific C and CN values provide a more accurate basis for predicting runoff and managing stormwater, allowing for tailored solutions that consider the local conditions of each catchment. While the limitations of using lumped parameters like C and CN in hydrological modeling are valid, using locally derived values is still useful for improving hydrological modeling and urban stormwater management. This has broader applicability to other urban areas globally, especially for areas where the use of distributed models can be challenging. These actionable insights are important for water engineers, urban planners, and policymakers as they seek to develop effective stormwater management strategies and prioritize nature-based infrastructures. As cities continue to expand and face the increasing challenges associated with extreme weather events and urban densification, the hydrologic benefits of urban green spaces as an element of nature-based infrastructures can help alleviate the pressure on urban drainage systems and potentially reduce the risk of pluvial flooding. Future studies can further explore and model different scenarios to investigate how the integration of trees with other stormwater management practices can maximize their functions and facilitate the implementation of nature-based solutions.

CRediT authorship contribution statement

Mark Bryan Alivio: Writing – original draft, Visualization, Investigation, Formal analysis, Conceptualization. **Matej Radinja:** Writing – review & editing, Investigation. **Mojca Šraj:** Writing – review & editing, Validation, Supervision. **Zoltán Gribovszki:** Writing – review & editing, Validation. **Nejc Bezak:** Writing – review & editing, Validation, Supervision, Conceptualization.

Funding

This study is part of ongoing research entitled "Microscale influence on runoff" supported by the Slovenian Research and Innovation Agency (N2-0313) and National Research, Development, and Innovation Office (OTKA project grant number SNN143972). The study was also carried out within the scope of the CELSA project entitled "Interception experimentation and modeling for enhanced impact analysis of nature-based solutions" and research program P2-0180: "Water Science and Technology, and Geotechnical Engineering: Tools and Methods for Process Analyses and Simulations, and Development of Technologies" through the Ph.D. grant of the first author that is financially supported by the Slovenian Research and Innovation Agency.

Declaration of competing interest

The authors declare that they have no known competing financial interests or personal relationships that could have appeared to influence the work reported in this paper.

Acknowledgment

The authors would like to acknowledge the Slovenian Environment Agency (ARSO) for making the data publicly available and the Slovenian Forestry Institute (Gozdarski inštitut Slovenije) for granting us the permission to access the meteorological data in the studied urban mixed forest. The authors also would like to thank the company JP VOKA SNAGA for providing the sewer system data and assistance with conducting flow measurements in the sewer system.

Data availability

Data will be made available on request.

References

Agonafir, C., Lakhankar, T., Khanbilvardi, R., Krakauer, N., Radell, D., Devineni, N., 2023. A review of recent advances in urban flood research. Water Security 19, 100141. https://doi.org/10.1016/j.wasec.2023.100141.

Alivio, M.B., Šraj, M., Bezak, N., 2023. Investigating the reduction of rainfall intensity beneath an urban deciduous tree canopy. Agric. for. Meteorol. 342, 109727. https://doi.org/10.1016/j.agrformet.2023.109727.

Arso, 2022. Current - Annual and Seasonal Maps. [WWW Document]. https://meteo.arso.gov.si/met/sl/climate/current/charts_seasons/.

ARSO. (Accessed on 23 October 2023). ARSO Meteorological Archive. Available online: https://meteo.arso.gov.si/met/sl/archive/.

Asce, 1992. Design and construction of urban stormwater management systems: ASCE Manuals and Reports of Engineering. Practice No. 77, ASCE-WEF. https://doi.org/10.1061/9780872628557.

ASCE. (1996). Hydrology Handbook (2nd ed.): ASCE Manuals and Reports on Engineering Practice No. 28. ASCE. https://doi.org/10.1061/9780784401385.

B.M. Tecnologie Industriali s.r.l. (20 of March 2020). Doppler sensors for KAPTOR Mini – BJONG User Manual. https://bmtecnologie.it/wp-content/uploads/2021/04/Doppler-Sensors-Kaptor-Mini-User-Manual-V0.2-20200330.pdf.

Baiamonte, G., 2020. A rational runoff coefficient for a revisited rational formula. Hydrol. Sci. J. 65 (1), 112–126. https://doi.org/10.1080/02626667.2019.1682150.

Banasik, K., & Woodward, D. (2010, June). Empirical determination of runoff curve number for a small agricultural watershed in Poland. In 2nd Joint Federal Interagency Conference, Las Vegas, NV, NV, June 27 – July 1. 2010, 10p. http://acwi.gov/sos/pubs/2ndJFIC/Contents/10E_Banasik_28_02_10.pdf.

Banasik, K., Krajewski, A., Sikorska, A., Hejduk, L., 2014. Curve Number estimation for a small urban catchment from recorded rainfall-runoff events. Archives of Environmental Protection 40 (3), 75–86. https://doi.org/10.2478/aep-2014-0032.

Bezak, N., Šraj, M., Rusjan, S., Mikoš, M., 2018. Impact of the rainfall duration and temporal rainfall distribution defined using the Huff curves on the hydraulic flood modelling results. Geosciences 8 (2), 69. https://doi.org/10.3390/geosciences8020069.

Birkinshaw, S.J., O'Donnell, G., Glenis, V., Kilsby, C., 2021. Improved hydrological modelling of urban catchments using runoff coefficients. J. Hydrol. 594, 125884. https://doi.org/10.1016/j.jhydrol.2020.125884.

Blume, T., Zehe, E., Bronstert, A., 2007. Rainfall—runoff response, event-based runoff coefficients and hydrograph separation. Hydrol. Sci. J. 52 (5), 843–862. https://doi.org/10.1623/hysj.52.5.843.

Boughton, W.C., 1989. A review of the USDA SCS curve number method. Soil Res. 27 (3), 511–523. https://doi.org/10.1071/SR9890511.

Bouwer, H., 2002. Artificial recharge of groundwater: hydrogeology and engineering. Hydrgeol. J. 10, 121–142. https://link.springer.com/content/pdf/10.1007/s10040-001-0182-4.pdf.

Callegari, G., Ferrari, E., Garfì, G., Iovino, F., Veltri, A., 2003. Impact of thinning on the water balance of a catchment in a Mediterranean environment. For. Chron. 79 (2), 301–306. https://doi.org/10.5558/tfc79301-2.

Chen, X., Parajka, J., Széles, B., Strauss, P., Blöschl, G., 2020a. Controls on event runoff coefficients and recession coefficients for different runoff generation mechanisms identified by three regression methods. Journal of Hydrology and Hydromechanics 68 (2), 155–169. https://doi.org/10.2478/johh-2020-0008.

Chen, X., Parajka, J., Széles, B., Strauss, P., Blöschl, G., 2020b. Spatial and temporal variability of event runoff characteristics in a small agricultural catchment. Hydrol. Sci. J. 65 (13), 2185–2195. https://doi.org/10.1080/02626667.2020.1798451.

Chin, D.A., 2019. Estimating peak runoff rates using the rational method. J. Irrig. Drain. Eng. 145 (6), 04019006. https://doi.org/10.1061/(ASCE)IR.1943-4774.00013.

Cleveland, T.G., Thompson, D.B., Fang, X., 2011. Use of the Rational and Modified Rational Method for Hydraulic Design, No. FHWA/TX–08/0–6070–1. Texas Tech University, Texas, USA.

Constantz, J., Thomas, C.L., Zellweger, G., 1994. Influence of diurnal variations in stream temperature on streamflow loss and groundwater recharge. Water Resour. Res. 30 (12), 3253–3264. https://doi.org/10.1029/94WR01968.

Constantz, J., Naranjo, R., Niswonger, R., Allander, K., Neilson, B., Rosenberry, D., Stonestrom, D., 2016. Groundwater exchanges near a channelized versus unmodified stream mouth discharging to a subalpine lake. Water Resour. Res. 52 (3), 2157–2177. https://doi.org/10.1002/2015WR017013.

Coron, L., Delaigue, O., Thirel, G., Dorchies, D., Perrin, C., Michel, C., 2023. airGR: Suite of GR Hydrological Models for Precipitation-Runoff Modelling. R Package Version 1 (7), 4. https://doi.org/10.15454/EX11NA, URL: https://CRAN.R-project.org/package=airGR.

Onset Computer Corporation. (2018). HOBO® Data Logger. HOBO® U20L Water Level Logger (U20L-0x) Manual. Bourne, MA, USA. Retrieved October 26, 2023 from https://www.onsetcomp.com/resources/documentation/17153-u20l-manual.

D'Asaro, F., Grillone, G., 2012. Empirical investigation of curve number method parameters in the Mediterranean area. J. Hydrol. Eng. 17 (10), 1141–1152. https://doi.org/10.1061/(ASCE)HE.1943-5584.0000570.

Demšar, J., Curk, T., Erjavec, A., Gorup, Č., Hočevar, T., Milutinovič, M., Zupan, B., 2013. Orange: data mining toolbox in Python. The Journal of Machine Learning Research 14 (1), 2349–2353. https://www.jmlr.org/papers/volume14/demsar13a/demsar13a.pdf.

Deshmukh, D.S., Chaube, U.C., Hailu, A.E., Gudeta, D.A., Kassa, M.T., 2013. Estimation and comparision of curve numbers based on dynamic land use land cover change, observed rainfall-runoff data and land slope. J. Hydrol. 492, 89–101. https://doi.org/10.1016/j.jhydrol.2013.04.001.

Deutscher, J., Kupec, P., Dundek, P., Holík, L., Machala, M., Urban, J., 2016. Diurnal dynamics of streamflow in an upland forested micro-watershed during short precipitation-free periods is altered by tree sap flow. Hydrol. Process. 30 (13), 2042–2049. https://doi.org/10.1002/hyp.10771.

Dhakal, N., Fang, X., Cleveland, T.G., Thompson, D.B., Asquith, W.H., Marzen, L.J., 2012. Estimation of volumetric runoff coefficients for Texas watersheds using land-use and rainfall-runoff data. J. Irrig. Drain. Eng. 138 (1), 43–54. https://doi.org/10.1061/(ASCE)IR.1943-4774.0000368.

do Amaral, F. R., Trung, T. N., Pellarin, T., & Gratiot, N., 2023. Datasets of high-resolution water level and discharge from the Saigon-Dong Nai estuary system impacted by a developing megacity, Ho Chi Minh City-Vietnam. Data Brief 48, 109147. https://doi.org/10.1016/j.dib.2023.109147.

Farran, M.M., Elfeki, A.M., 2020. Variability of the asymptotic curve number in mountainous undeveloped arid basins based on historical data: case study in Saudi Arabia. J. Afr. Earth Sc. 162, 103697. https://doi.org/10.1016/j.jafrearsci.2019.103697.

Fassman-Beck, E., Hunt, W., Berghage, R., Carpenter, D., Kurtz, T., Stovin, V., Wadzuk, B., 2016. Curve number and runoff coefficients for extensive living roofs. J. Hydrol. Eng. 21 (3), 04015073. https://doi.org/10.1061/(ASCE)HE.1943-5584.0001318.

Gajbhiye, S., Mishra, S.K., Pandey, A., 2013. Effects of seasonal/monthly variation on runoff curve number for selected watersheds of Narmada basin. Int. J. Environ. Sci. 3 (6), 2019–2030. https://doi.org/10.6088/ijes.2013030600022.

E. Gómez-Baggethun et al. Urban Ecosystem Services . In: Elmqvist, T., et al. Urbanization, Biodiversity and Ecosystem Services: Challenges and Opportunities 2013 Springer Dordrecht 10.1007/978-94-007-7088-1_11.

Gonzalez, A., Temimi, M., Khanbilvardi, R., 2015. Adjustment to the curve number (NRCS-CN) to account for the vegetation effect on hydrological processes. Hydrol. Sci. J. 60 (4), 591–605. https://doi.org/10.1080/02626667.2014.898119.

Gribovszki, Z., Kalicz, P., Kucsara, M., 2006. Streamflow Characteristics of Two Forested Catchments in Sopron Hill. Acta Silvatica et Lignaria Hungarica 2, 81–92. https://journal.uni-sopron.hu/index.php/aslh/article/view/Acta-Silvatica-Lignaria-Hungarica-2006-Vol02-081-091.

Grimaldi, S., Petroselli, A., 2015. Do we still need the rational formula? An alternative empirical procedure for peak discharge estimation in small and ungauged basins. Hydrol. Sci. J. 60 (1), 67–77. https://doi.org/10.1080/02626667.2014.880546.

Gundalia, M., Dholakia, M., 2014. Impact of monthly curve number on daily runoff estimation for Ozat catchment in India. Open Journal of Modern Hydrology 4 (04), 144. https://doi.org/10.4236/ojmh.2014.44014.

Hao, L., Sun, G., Liu, Y., Wan, J., Qin, M., Qian, H., Chen, J., 2015. Urbanization dramatically altered the water balances of a paddy field-dominated basin in southern China. Hydrol. Earth Syst. Sci. 19 (7), 3319–3331. https://doi.org/10.5194/hess-19-3319-2015.

Hawkins, R.H., 1993. Asymptotic determination of runoff curve numbers from data. J. Irrig. Drain. Eng. 119 (2), 334–345. https://doi.org/10.1061/(ASCE)0733-9437(1993)119:2(334).

Hawkins, R.H., Ward, T.J., Woodward, D.E., Van Mullem, J.A., (Eds.)., 2008. November). State of the practice. American Society of Civil Engineers, Curve number hydrology http://ndl.ethernet.edu.et/bitstream/123456789/55128/1/410.pdf.

Hayes, D.C., Young, R.L., 2006. Comparison of Peak Discharge and Runoff Characteristic Estimates from the Rational Method to Field Observations for Small Basins in Central Virginia No, 2005–5254. https://doi.org/10.3133/sir20055254.

Hjelmfelt Jr, A.T., 1980. Empirical investigation of curve number technique. J. Hydraul. Div. 106 (9), 1471–1476. https://doi.org/10.1061/JYCEAJ.0005506.

Ibrahim, S., Brasi, B., Yu, Q., Siddig, M., 2022. Curve number estimation using rainfall and runoff data from five catchments in Sudan. Open Geosciences 14 (1), 294–303. https://doi.org/10.1515/geo-2022-0356.

Jaafar, H. H., Ahmad, F. A., & El Beyrouthy, N. (2019). GCN250, new global gridded curve numbers for hydrologic modeling and design. Scientific data, 6(1), 145. https://doi.org/10.1038/s41597-019-0155-xKermavnar, J., & Vilhar, U. (2017). Canopy precipitation interception in urban forests in relation to stand structure. Urban Ecosystems, 20, 1373-1387. https://doi.org/10.1007/s11252-017-0689-7.

Kobold, M., & Sušelj, K. (2004). Padavinske napovedi in njihova nezanesljivost v hidrološkem prognoziranju. V: Raziskave s področja geodezije in geofizike, 61-75. https://fgg-web.fgg.uni-lj.si/SUGG/referati/2005/SZGG_05_Kobold_Suselj.pdf.

Kong, X., Zhang, X., Xu, C., Hauer, R.J., 2021. Review on urban forests and trees as nature-based solutions over 5 years. Forests 12 (11), 1453. https://doi.org/10.3390/f12111453.

Krevs, M., Djordjević, D., Pichler-Milanović, N. (Eds.), 2010. Challenges of Spatial Development of Ljubljana and Belgrade. Znanstvena založba Filozofske fakultete, Oddelek za geografijo https://pdfs.semanticscholar.org/bca0/afdb93efb4acf12b7f18730944b7066439b1.pdf.

Lal, M., Mishra, S.K., Pandey, A., Pandey, R.P., Meena, P.K., Chaudhary, A., Kumar, Y., 2017. Evaluation of the Soil Conservation Service curve number methodology using data from agricultural plots. Hydrgeol. J. 25 (1), 151. https://doi.org/10.1007/s10040-016-1460-5.

Li, C., Liu, M., Hu, Y., Shi, T., Qu, X., Walter, M.T., 2018. Effects of urbanization on direct runoff characteristics in urban functional zones. Sci. Total Environ. 643, 301–311. https://doi.org/10.1016/j.scitotenv.2018.06.211.

Lian, H., Yen, H., Huang, J.C., Feng, Q., Qin, L., Bashir, M.A., Liu, H., 2020. CN-China: Revised runoff curve number by using rainfall-runoff events data in China. Water Res. 177, 115767. https://doi.org/10.1016/j.watres.2020.115767.

Lundquist, J.D., Cayan, D.R., 2002. Seasonal and spatial patterns in diurnal cycles in streamflow in the western United States. J. Hydrometeorol. 3 (5), 591–603. https://doi.org/10.1175/1525-7541(2002)003<0591:SASPID>2.0.CO;2.
Lyne, V., Hollick, M., 1979. September). Stochastic Time-Variable Rainfall-Runoff Modelling. in Institute of Engineers Australia National Conference Vol. 79(10, 89–93.
Machado, R.E., Cardoso, T.O., Mortene, M.H., 2022. Determination of runoff coefficient (C) in catchments based on analysis of precipitation and flow events. International Soil and Water Conservation Research 10 (2), 208–216. https://doi.org/10.1016/j.iswcr.2021.09.001.
Marelle, L., Myhre, G., Steensen, B.M., Hodnebrog, Ø., Alterskjær, K., Sillmann, J., 2020. Urbanization in megacities increases the frequency of extreme precipitation events far more than their intensity. Environ. Res. Lett. 15 (12), 124072. https://doi.org/10.1088/1748-9326/abcc8f.
McCuen, R.H., 2005. Hydrologic analysis and design (4th edition). Prentice-Hall, Upper Saddler River, NJ, pp. 376–378.
Meißl, G., Zieher, T., Geitner, C., 2020. Runoff response to rainfall events considering initial soil moisture–Analysis of 9-year records in a small Alpine catchment (Brixenbach valley, Tyrol, Austria). J. Hydrol.: Reg. Stud. 30, 100711. https://doi.org/10.1016/j.ejrh.2020.100711.
Merz, R., Blöschl, G., 2009. A regional analysis of event runoff coefficients with respect to climate and catchment characteristics in Austria. Water Resour. Res. 45 (1). https://doi.org/10.1029/2008WR007163.
Miao, S., Chen, F., Li, Q., Fan, S., 2011. Impacts of urban processes and urbanization on summer precipitation: A case study of heavy rainfall in Beijing on 1 August 2006. J. Appl. Meteorol. Climatol. 50 (4), 806–825. https://doi.org/10.1175/2010JAMC2513.1.
Miller, J. J., Mizell, S. A., French, R. H., Meadows, D. G., & Young, M. H. (2005). Channel Transmission Loss Studies During Ephemeral Flow Events: ER-5-3 Channel and Cambric Ditch, Nevada Test Site, Nye County, Nevada (No. DOE/NV/13609-42). Desert Research Institute, Nevada System of Higher Education. https://www.osti.gov/servlets/purl/876752.
Mishra, S. K., Suresh Babu, P., & Singh, V. P. (2007). SCS-CN method revisited. Advances in Hydraulics and Hydrology; Water Resources Publications: Littleton, CO, USA. https://www.researchgate.net/publication/230822228_SCS-CN_method_revisitedMuche, M. E., Hutchinson, S. L., Hutchinson, J. S., & Johnston, J. M. (2019). Phenology-adjusted dynamic curve number for improved hydrologic modeling. Journal of environmental management, 235, 403-413. https://doi.org/10.1016/j.jenvman.2018.12.115.
Mishra, S.K., Singh, V.P., 2004. Long-term hydrological simulation based on the Soil Conservation Service curve number. Hydrol. Process. 18 (7), 1291–1313. https://doi.org/10.1002/hyp.1344.
Nastran, M., Regina, H., 2016. Advancing urban ecosystem governance in Ljubljana. Environ Sci Policy 62, 123–126.
Norbiato, D., Borga, M., Merz, R., Blöschl, G., Carton, A., 2009. Controls on event runoff coefficients in the eastern Italian Alps. J. Hydrol. 375 (3–4), 312–325. https://doi.org/10.1016/j.jhydrol.2009.06.044.
Oliveira, P.T.S., Nearing, M.A., Hawkins, R.H., Stone, J.J., Rodrigues, D.B.B., Panachuki, E., Wendland, E., 2016. Curve number estimation from Brazilian Cerrado rainfall and runoff data. J. Soil Water Conserv. 71 (5), 420–429. https://doi.org/10.2489/jswc.71.5.420.
Orta-Ortiz, M.S., Geneletti, D., 2022. What variables matter when designing nature-based solutions for stormwater management? A review of impacts on ecosystem services. Environ. Impact Assess. Rev. 95, 106802. https://doi.org/10.1016/j.eiar.2022.106802.
Oudin, L., Hervieu, F., Michel, C., Perrin, C., Andréassian, V., Anctil, F., Loumagne, C., 2005. Which potential evapotranspiration input for a lumped rainfall-runoff model? Part 2 - Towards a simple and efficient potential evapotranspiration model for rainfall-runoff modelling. J. Hydrol. 303 (1–4), 290–306. https://doi.org/10.1016/j.jhydrol.2004.08.026.
Penna, D., Tromp-van Meerveld, H.J., Gobbi, A., Borga, M., Dalla Fontana, G., 2011. The influence of soil moisture on threshold runoff generation processes in an alpine headwater catchment. Hydrol. Earth Syst. Sci. 15 (3), 689–702. https://doi.org/10.5194/hess-15-689-2011.
R Core Team, 2021. R: A language and environment for statistical computing. R Foundation for Statistical Computing, Vienna, Austria https://www.R-project.org/.
Radinja, M., Vidmar, I., Atanasova, N., Mikoš, M., Šraj, M., 2019. Determination of spatial and temporal variability of soil hydraulic conductivity for urban runoff modelling. Water 11 (5), 941. https://doi.org/10.3390/w11050941.
Radinja, M., Škerjanec, M., Šraj, M., Džeroski, S., Todorovski, L., Atanasova, N., 2021. Automated modelling of urban runoff based on domain knowledge and equation discovery. J. Hydrol. 603, 127077. https://doi.org/10.1016/j.jhydrol.2021.127077.
Rammal, M., Berthier, E., 2020. Runoff losses on urban surfaces during frequent rainfall events: a review of observations and modeling attempts. Water 12 (10), 2777. https://doi.org/10.3390/w12102777.
Redfern, T. W. (2017). Monitoring, Understanding and Modelling Rainfall-Runoff Behaviour in Two Small Residential Urban Catchments [Dissertation]. The University of Liverpool (United Kingdom). https://www.proquest.com/docview/2501876342?pq-origsite=gscholar&fromopenview=true.
Rodríguez-Blanco, M.L., Taboada-Castro, M.M., Taboada-Castro, M.T., 2012. Rainfall–runoff response and event-based runoff coefficients in a humid area (northwest Spain). Hydrol. Sci. J. 57 (3), 445–459. https://doi.org/10.1080/02626667.2012.666351.
Ronan, A.D., Prudic, D.E., Thodal, C.E., Constantz, J., 1998. Field study and simulation of diurnal temperature effects on infiltration and variably saturated flow beneath an ephemeral stream. Water Resour. Res. 34 (9), 2137–2153. https://doi.org/10.1029/98WR01572.
Rusjan, S., Fazarinc, R., Mikoš, M., 2003. River rehabilitation of urban watercourses on the example of the Glinščica river in Ljubljana. Acta Hydrotechnica 21 (34), 1–22. https://actahydrotechnica.fgg.uni-lj.si/en/paper/a34sr.
Salazar, S., Francés, F., Komma, J., Blume, T., Francke, T., Bronstert, A., Blöschl, G., 2012. A comparative analysis of the effectiveness of flood management measures based on the concept of" retaining water in the landscape" in different European hydro-climatic regions. Nat. Hazards Earth Syst. Sci. 12 (11), 3287–3306. https://doi.org/10.5194/nhess-12-3287-2012.
Schwab, M., Klaus, J., Pfister, L., Weiler, M., 2016. Diel discharge cycles explained through viscosity fluctuations in riparian inflow. Water Resour. Res. 52 (11), 8744–8755. https://doi.org/10.1002/2016WR018626.
Singh, P., Mishra, S., 2019. Determination of curve number and estimation of runoff using Indian experimental rainfall and runoff data. J. Spat. Hydrol. 13 (1). https://scholarsarchive.byu.edu/josh/vol13/iss1/2.
Soulis, K.X., 2018. Estimation of SCS Curve Number variation following forest fires. Hydrol. Sci. J. 63 (9), 1332–1346. https://doi.org/10.1080/02626667.2018.1501482.
Soulis, K.X., Valiantzas, J.D., Dercas, N., Londra, P.A., 2009. Investigation of the direct runoff generation mechanism for the analysis of the SCS-CN method applicability to a partial area experimental watershed. Hydrol. Earth Syst. Sci. 13 (5), 605–615.
Strapazan, C., Irimuș, I.A., Șerban, G., Man, T.C., Sassebes, L., 2023. Determination of Runoff Curve Numbers for the Growing Season Based on the Rainfall-Runoff Relationship from Small Watersheds in the Middle Mountainous Area of Romania. Water 15 (8), 1452. https://doi.org/10.3390/w15081452.
Sun, G., Lockaby, B.G., 2012. Water Quantity and Quality at the Urban-Rural Interface. In: Laband, D.N., Lockaby, B.G., Zipperer, W. (Eds.), Urban-Rural Interfaces: Linking People and Nature (chap, 3. American Society of Agronomy, Crop Science Society of America, Soil Science Society of America, Madison, Wisconsin, pp. 29–48. https://doi.org/10.2136/2012.urban-rural.c3.
Svetina, J., Prestor, J., Šraj, M., 2023. Infiltration Measurements during Dry Conditions in an Urban Park in Ljubljana. Slovenia. Water 15 (20), 3635. https://doi.org/10.3390/w15203635.
Taguas, E.V., Nadal-Romero, E., Ayuso, J.L., Casalí, J., Cid, P., Dafonte, J., Zabaleta, A., 2017. Hydrological signatures based on event runoff coefficients in rural catchments of the Iberian Peninsula. Soil Sci. 182 (5), 159–171. https://doi.org/10.1097/SS.0000000000000210.
Tedela, N. H., Rasmussen, T. C., & McCutcheon, S. C. (2007). Effects of seasonal variation on runoff curve number for selected watersheds of Georgia—preliminary study. In Proc., Georgia Water Resources Conference. http://www.hydrology.uga.edu/rasmussen/pubs/GWRC2007a.pdf.
Tedela, N.H., McCutcheon, S.C., Rasmussen, T.C., Hawkins, R.H., Swank, W.T., Campbell, J.L., Tollner, E.W., 2012a. Runoff curve numbers for 10 small forested watersheds in the mountains of the eastern United States. J. Hydrol. Eng. 17 (11), 1188–1198. https://doi.org/10.1061/(ASCE)HE.1943-5584.0000436.
Tedela, N.H., McCutcheon, S.C., Campbell, J.L., Swank, W.T., Adams, M.B., Rasmussen, T.C., 2012b. Curve numbers for nine mountainous eastern United States watersheds: Seasonal variation and forest cutting. J. Hydrol. Eng. 17 (11), 1199–1203. https://doi.org/10.1061/(ASCE)HE.1943-5584.0000437.
Thomas, C., 2017. A case study of runoff coefficients for urban areas with different drainage systems [Master's thesis]. Water and Environmental Engineering, Lund University, Lund, Sweden, Department of Chemical Engineering https://lup.lub.lu.se/luur/download?func=downloadFile&recordOId=8917902&fileOId=8917929.
Toreti, A., Bavera, D., Acosta Navarro, J., Cammalleri, C., de Jager, A., Di Ciollo, C., Hrast Essenfelder, A., Maetens, W., Magni, D., Masante, D., Mazzeschi, M., Niemeyer, S., Spinoni, J., 2022. Drought in Europe August 2022. Publications Office of the European Union, Luxembourg. https://doi.org/10.2760/264241.
Uber, M., Vandervaere, J.P., Zin, I., Braud, I., Heistermann, M., Legoût, C., Nord, G., 2018. How does initial soil moisture influence the hydrological response? A case study from southern France. Hydrol. Earth Syst. Sci. 22 (12), 6127–6146. https://doi.org/10.5194/hess-22-6127-2018.
United States Department of Agriculture (USDA), 1986. Urban Hydrology for Small Watersheds (TR-55), 2nd Ed. USDA-SCS, Washington, D.C. https://directives.sc.egov.usda.gov/OpenNonWebContent.aspx?content=22162.wba.
United States Department of Agriculture-Natural Resources Conservation Service (USDA-NRCS), 2004. 210-National Engineering Handbook, Part 630, Hydrology, Chapter 9. Hydrologic Soil-Cover Complexes, USDA-NRCS, Washington, D.C. https://directives.sc.egov.usda.gov/OpenNonWebContent.aspx?content=17758.wba.
Van Mullem, J.A., Woodward, D.E., Hawkins, R.H., Hjelmfelt, A.T., Quan, Q.D., 2002. July). Runoff Curve Number Method: beyond the Handbook. Las Vegas, Nevada.
Velpuri, N.M., Senay, G.B., 2013. Analysis of long-term trends (1950–2009) in precipitation, runoff and runoff coefficient in major urban watersheds in the United States. Environ. Res. Lett. 8 (2), 024020. https://doi.org/10.1088/1748-9326/8/2/024020.
Viglione, A., Merz, R., Blöschl, G., 2009. On the role of the runoff coefficient in the mapping of rainfall to flood return periods. Hydrol. Earth Syst. Sci. 13 (5), 577–593. https://doi.org/10.5194/hess-13-577-2009.
Wilson, L.E., Ramirez-Avila, J.J., Hawkins, R.H., 2017. Runoff curve number estimation for agricultural systems in the southern region of USA. In: In World Environmental and Water Resources Congress 2017, pp. 353–366.
Woodward, D.E., Hawkins, R.H., Jiang, R., Hjelmfelt Jr, A.T., Van Mullem, J.A., Quan, Q. D., 2003. June). Runoff curve number method: Examination of the initial abstraction ratio. In: In World Water & Environmental Resources Congress 2003, pp. 1–10. https://doi.org/10.1061/40685(2003)308.

Woodward, D.E., Scheer, C.C., Hawkins, R.H., 2006. Curve number update used for runoff calculation. Annals of Warsaw Agricultural University-SGGW. Land Reclamation 37, 33–42. https://agro.icm.edu.pl/agro/element/bwmeta1.element.agro-article-507151c5-1759-4ef0-81c1-9ac462b3ee78.

Xiong, J., Yin, J., Guo, S., He, S., Chen, J., 2022. Annual runoff coefficient variation in a changing environment: a global perspective. Environ. Res. Lett. 17 (6), 064006. https://doi.org/10.1088/1748-9326/ac62ad.

Young, C.B., McEnroe, B.M., Rome, A.C., 2009. Empirical determination of rational method runoff coefficients. J. Hydrol. Eng. 14 (12), 1283–1289. https://doi.org/10.1061/(ASCE)HE.1943-5584.00001.

Zabret, K., & Šraj, M. (2019a). Rainfall interception by urban trees and their impact on potential surface runoff. CLEAN–Soil, Air, Water, 47(8), 1800327. https://doi.org/10.1002/clen.201800327Zabret, K., & Šraj, M. (2019b). Evaluating the influence of rain event characteristics on rainfall interception by urban trees using multiple correspondence analysis. Water, 11(12), 2659. https://doi.org/10.3390/w11122659.

Zabret, K., Šraj, M., 2018. Spatial variability of throughfall under single birch and pine tree canopies. Acta Hydrotechnica 31, 1–20. https://doi.org/10.15292/acta.hydro.2018.01.

Zabret, K., Rakovec, J., Šraj, M., 2018. Influence of meteorological variables on rainfall partitioning for deciduous and coniferous tree species in urban area. J. Hydrol. 558, 29–41. https://doi.org/10.1016/j.jhydrol.2018.01.025.

Zabret, K., Šraj, M., 2021. Relation of influencing variables and weather conditions on rainfall partitioning by birch and pine trees. J. Hydrol. Hydromechanics 69, 456–466. https://doi.org/10.2478/johh-2021-0023.

Zabret, K., Lebar, K., Šraj, M., 2023. Temporal response of urban soil water content in relation to the rainfall and throughfall dynamics in the open and below the trees. Journal of Hydrology and Hydromechanics 71 (2), 210–220. https://doi.org/10.2478/johh-2023-0007.

Zaki, M.J., Meira, W., 2014. Data mining and analysis: fundamental concepts and algorithms. Cambridge University Press.

Zhang, Z., Chen, X., Huang, Y., Zhang, Y., 2014. Effect of catchment properties on runoff coefficient in a karst area of southwest China. Hydrol. Process. 28 (11), 3691–3702. https://doi.org/10.1002/hyp.9920.

Zheng, Y., Coxon, G., Woods, R., Li, J., Feng, P., 2023. Controls on the spatial and temporal patterns of rainfall-runoff event characteristics-a large sample of catchments across Great Britain. Water Resour. Res. e2022WR033226. https://doi.org/10.1029/2022WR033226.